Differentiation of neurospheres

The secondary neurospheres that were cultured in the presence of HGF only, FGF-2 + EGF, or FGF-2 + EGF + HGF were rinsed in growth medium without any growth factors, and dissociated with a fire-polished pipet. Dissociated cells (1×10^5 cells) were plated onto poly-D-lysine-coated coverslips in 24-well plates (Falcon). To determine the effects of HGF on differentiation of NSCs, each well contained 1% fetal bovine serum (FBS) and 20 ng/ml HGF or only 1% FBS. The cells were fixed with 4% paraformaldehyde in PBS containing 4% sucrose after 7 days.

Antibody

Primary antibodies (final dilution, source) included mouse monoclonal antibody to nestin (1:500; Chemicon), mouse monoclonal antibody to microtubule-associated protein 2 (MAP-2, 1:500; Sigma–Aldrich), rabbit polyclonal antibody to glial fibrillary acidic protein (GFAP, 1:500; DAKO), mouse IgM monoclonal antibody to O_4 (1:20; Chemicon), rabbit polyclonal antibody to c-Met (1:100; Santa Cruz), and mouse monoclonal antibody to bromodeoxyuridine (BrdU) (1:2; Becton Dickinson Immunocytometry Systems). Secondary antibodies were fluorescein (FITC)-conjugated goat anti-mouse IgG (1:200; Biosource International), rhodamine (TRITC)-conjugated goat anti-mouse IgG (1:200; Molecular Probes), fluorescein-conjugated affinity-purified goat antibody to mouse IgM (1:200; ICN Pharmaceuticals), FITC-conjugated goat anti- rabbit IgG (1:200; MBL, Japan), and AMCA -conjugated goat anti-rabbit IgG (1:200; Chemicon).

Immunocytochemistry

The cells were fixed in 4% paraformaldehyde in PBS containing 4% sucrose for 30 min. For c-Met immunofluorescence staining, the cells were fixed in 75% cold methanol, washed in PBS and incubated in blocking solution (2% skim milk, 1% normal goat serum, 0.2% BSA, and 0.2% Triton X-100 in PBS) for 2 h. For triple-label immunostaining, primary antibodies (anti-MAP-2, anti-GFAP) were diluted in PBS containing 2% skim milk and 0.2% Triton X-100. The cells on coverslips were incubated for 2 h at 37°C, and secondary antibodies were added and incubated for an additional 2 h at 37°C. The cells were subsequently incubated with mouse IgM monoclonal antibody to O_4 for 1 h at 37°C, and then incubated with fluorescein-conjugated affinity-purified goat antibody to mouse IgM for another 1 h at 37°C. Finally, coverslips were washed twice with PBS, then Hoechst (10 μM) was added for 5 min at room temperature, and the coverslips were washed twice in PBS. A rapid water wash preceded the mounting on glass slides with Vectoshield (Vector Laboratories).

BrdU labeling and detection

Incorporation of BrdU was determined by adding 10 μM BrdU (Sigma-Aldrich) to cultures of secondary neurospheres grown for 5 days in the presence of various growth factors. At 2 h after BrdU addition, the cells were collected, washed with culture medium, mechanically dissociated, resuspended in differentiation medium (growth medium plus 1% FBS), and plated onto poly-D-lysine-coated coverslips in 24-well plates (Falcon). The cells were fixed 2 h later with cold 75% methanol for 20 min, denatured with 2 M HCl for 30 min, and washed twice with PBS. The cells were incubated with anti-BrdU for 30 min at 37°C, and then washed with PBS two times. The cells were incubated with FITC-conjugated goat anti-mouse IgG for 30 min at 37°C. Finally, the cells were washed twice with PBS, 0.04 mg/ml propidium iodide (Molecular Probes) was added for 5 min at room temperature, and the cells were washed twice in PBS.

TUNEL assay

To evaluate the number of apoptotic cells in the growing condition, secondary neurospheres were fixed in 1% paraformaldehyde. To evaluate the number of apoptotic cells in the differentiating condition, cells were plated on poly-D-lysine-coated coverslips in 24-well plates (Falcon) in differentiation medium for 6 days, and then fixed in 1% paraformaldehyde. Those cells were stained using a TUNEL kit (ApopTag fluorescein kits, Intergen).

Cell counts and statistical analysis

Fluorescence was detected and photographed under a fluorescence microscope with a high-resolution digital camera (DMRA, Q-Fish system, Leica, Germany). The immunoreactivity and number of cells in 10 visual fields (50–100 cells per field) per coverslip were evaluated in a randomized fashion. Unpaired t tests were used to assess differences between experiments. All results are expressed as means ± SEM.

Acknowledgments

We thank Dr. T. Takami and Dr. M. Saio in the Department of Cellular Pathology Division of Bioregulatory Medicine, for the use of fluorescence microscopy.

References

Achim, C.L., Katyal, S., Wiley, C.A., Shiratori, M., Wang, G., Oshika, E., Petersen, B.E., Li, J.M., Michalopoulos, G.K., 1997. Expression of HGF and c-Met in the developing and adult brain. Dev. Brain. Res. 102, 299–303.

Ahmed, S., Reynolds, B.A., Weiss, S., 1995. BDNF enhances the differentiation but not the survival of CNS stem cell-derived neuronal precursors. J. Neurosci. 15, 5765–5778.

Armstrong, R.J., Watts, C., Svendsen, C.N., Dunnctt, S.B., Rosser, A.E., 2000. Survival, neuronal differentiation, and fiber outgrowth of propagated human neural precursor grafts in an animal model of Huntington's disease. Cell Transplant. 9, 55–64.

Arsenijevic, Y., Weiss, S., 1998. IGF-1 is a differentiation factor for postmitotic CNS stem cell-derived neuronal precursors: distinct actions from those of BDNF. J. Neurosci. 18, 2118–2128.

Arsenijevic, Y., Weiss, S., Schneider, B., Aebischer, P., 2001. Insulin-like growth factor-1 is necessary for neural stem cell proliferation and demonstrates distinct actions of epidermal growth factor and fibroblast growth factor-2. J. Neurosci. 21, 7194–7202.

Blaschke, A.J., Staley, K., Chun, J., 1996. Widespread programmed cell death in proliferative and postmitotic regions of the fetal cerebral cortex. Development 122, 1165–1174.

Bonni, A., Sun, Y., Nadal-Vicens, M., Bhatt, A., Frank, D., Rozovsky, I., Stahl, N., Yancopoulos, G., Greenberg, M., 1997. Regulation of gliogenesis in the central nervous system by the JAK-STAT signaling pathway. Science 278, 477–483.

Ebens, A., Brose, K., Leonardo, E.D., Hanson Jr., M.G., Bladt, F., Birchmeier, C., Barres, B.A., Tessier-Lavigne, M., 1996. Hepatocyte growth factor/scatter factor is an axonal chemoattractant and a neurotrophic factor for spinal motor neurons. Neuron 17, 1157–1172.

Erlandsson, A., Enarsson, M., Forsberg-Nilsson, K., 2001. Immature neurons from CNS stem cells proliferate in response to platelet-derived growth factor. J. Neurosci. 21, 3483–3491.

Hamanoue, M., Takemoto, N., Matsumoto, K., Nakamura, T., Nakajima, K., Kohsaka, S., 1996. Neurotrophic effect of hepatocyte growth factor on central nervous system neurons in vitro. J. Neurosci. Res. 43, 554–564.

Honda, S., Kagoshima, M., Wanaka, A., Tohyama, M., Matsumoto, K., Nakamura, T., 1995. Localization and functional coupling of HGF and c-Met/HGF receptor in rat brain: implication as neurotrophic factor. Mol. Brain. Res. 32, 197–210.

Johe, K.K., Hazel, T.G., Muller, T., Dugich Djordjevic, M.M., McKay, R.D.G., 1996. Single factors direct the differentiation of stem cells from the fetal and adult central nervous system. Genes Dev. 10, 3129–3140.

Jung, W., Castren, E., Odentha, M., Vande Woude, G.F., Ishii, T., Dienes, H.P., Lindholm, D., Schirmacher, P., 1994. Expression and functional interaction of hepatocyte growth factor-scatter factor and its receptor c-met in mammalian brain. J. Cell. Biol. 126, 485–494.

Maina, F., Klein, R., 1999. Hepatocyte growth factor, a versatile signal for developing neurons. Nat. Neurosci. 2, 213–217.

Matsumoto, K., Nakamura, T., 1997. Hepatocyte growth factor (HGF) as a tissue organizer for organogenesis and regeneration. Biochem. Biophys. Res. Commun. 239, 639–644.

McKay, R., 1997. Stem cells in the central nervous system. Science 276, 66–71.

Morrison, S.J., Shah, N.M., Anderson, D.J., 1997. Regulatory mechanisms in stem cell biology. Cell 88, 287–298.

Nakamura, T., Nishizawa, T., Hagiya, M., Seki, T., Shimonishi, M., Sugimura, A., Tashiro, K., Shimizu, S., 1989. Molecular cloning and expression of human hepatocyte growth factor. Nature 342, 440–443.

Nieto, M., Schuurmans, C., Britz, O., Guillemot, F., 2001. Neural bHLH genes control the neuronal versus glial fate decision in cortical progenitors. Neuron 29, 401–413.

Novak, K.D., Prevette, D., Wang, S., Gould, T.W., Oppenheim, R.W., 2000. Hepatocyte growth factor/scatter factor is a neurotrophic survival factor for lumber but not for other somatic motorneurons in chick embryo. J. Neurosci. 20, 326–337.

Okano, H., 2002. Stem cell biology of the central nervous system. J. Neurosci. Res. 69, 698–707.

Oppenheim, R.W., 1991. Cell death during development of the nervous system. Annu. Rev. Neurosci. 14, 453–501.

Palmer, T.D., Takahashi, J., Gage, F.H., 1997. The adult rat hippocampus contains primordial neural stem cells. Mol. Cell. Neurosci. 8, 389–404.

Qian, X., Shen, Q., Goderie, S.K., He, W., Capela, A., Davis, A.A., Temple, S., 2000. Timing of CNS cell generation: a programmed sequence of neuron and glial cell production from isolated murine cortical stem cells. Neuron 28, 69–80.

Reynolds, B.A., Weiss, S., 1992. Generation of neurons and astrocytes from isolated cells of the adult mammalian central nervous system. Science 255, 1707–1710.

Reynolds, B.A., Weiss, S., 1996. Clonal and population analyses demonstrate that an EGF-responsive mammalian embryonic CNS precursor is a stem cell. Dev. Biol. 175, 1–13.

Shimazaki, T., Shingo, T., Weiss, S., 2001. The ciliary neurotrophic factor/leukemia inhibitory factor/gp 130 receptor complex operates in the maintenance of mammalian forebrain neural stem cells. J. Neurosci. 21, 7642–7653.

Streit, A., Sockanathan, S., Perez, L., Rex, M., Scotting, P.J., Sharpe, P.T., Lovell-Badge, R., Stern, C.D., 1997. Prevention of the loss of competence for neural induction: HGF/SF, L5 and Sox-2. Development 124, 1191–1202.

Svendsen, C.N., Caldwell, M.A., 2000. Neural stem cells in the developing central nervous system: implications for cell therapy through transplantation. Prog. Brain. Res. 127, 13–24.

Svendsen, C.N., Caldwell, M.A., Shen, J., ter Borg, M., Rosser, A.E., Tyers, P., Karmiol, S., Dunnett, S.B., 1997. Long-term survival of human central nervous system progenitor cells transplanted into a rat model of Parkinson's disease. Exp. Neurol. 148, 135–146.

Temple, S., Davis, A.D., 1994. Isolated rat cortical progenitor cells are maintained in division in vitro by membrane-associated factors. Development 120, 999–1008.

Thomaidou, D., Mione, M.C., Cavanagh, J.F., Parnavelas, J.G., 1997. Apoptosis and its relation to the cell cycle in the developing cerebral cortex. J. Neurosci. 17, 1075–1085.

Tomita, K., Moriyoshi, K., Nakanishi, S., Guillemot, F., Kageyama, R., 2000. Mammalian achaete-scute and atonal homologs regulate neuronal versus glial fate determination in the central nervous system. EMBO. J. 19, 5460–5472.

Tropepe, V., Craig, C.G., Morshead, C.M., van der Kooy, D., 1997. Transforming growth factor-a null and senescent mice show decreased neural progenitor cell proliferation in the forebrain subependyma. J. Neurosci. 17, 7850–7859.

Tropepe, V., Shibilia, M., Ciruna, B.G., Rossant, J., Wagner, E.F., van der Kooy, D., 1999. Distinct neural stem cells proliferate in response to EGF and FGF in developing mouse telencephalon. Dev. Biol. 208, 166–188.

Weiss, S., Dunne, C., Hewson, J., Wohl, C., Wheatley, M., Peterson, A.C., Reynolds, B.A., 1996. Multipotent CNS stem cells are present in the adult mammalian spinal cord and ventricular neuroaxis. J. Neurosci. 16, 7599–7609.

Yoshimura, S., Takagi, Y., Harada, J., Teramoto, T., Thomas, S.S., Waeber, C., Bakowska, J.C., Breakefield, X.O., Moskowitz, M.A., 2001. FGF-2 regulation of neurogenesis in adult hippocampus after brain injury. Proc. Natl. Acad. Sci. USA 98, 5874–5876.

Thyroid hormone-upregulated expression of Musashi-1 is specific for progenitor cells of the adult epithelium during amphibian gastrointestinal remodeling

Atsuko Ishizuya-Oka[1,*], Katsuhiko Shimizu[1], Shin-ichi Sakakibara[1], Hideyuki Okano[2] and Shuichi Ueda[1]

[1]Department of Histology and Neurobiology, Dokkyo University School of Medicine, Mibu, Tochigi 321-0293, Japan
[2]Department of Physiology, Keio University School of Medicine, Shinjuku-ku, Tokyo 160-8582, Japan
*Author for correspondence (e-mail: i-oka@dokkyomed.ac.jp)

Accepted 15 April 2003
Journal of Cell Science 116, 3157-3164 © 2003 The Company of Biologists Ltd
doi:10.1242/jcs.00616

Summary

In the amphibian gastrointestine during metamorphosis, the primary (larval) epithelium undergoes apoptosis. By contrast, a small number of undifferentiated cells including stem cells actively proliferate and differentiate into the secondary (adult) epithelium that resembles the mammalian counterpart. In the present study, to clarify whether Musashi-1 (Msi-1), an RNA-binding protein, serves as a marker for progenitor cells of the adult epithelium, we chronologically examined Msi-1 expression in the *Xenopus laevis* gastrointestine by using in situ hybridization and immunohistochemistry. Similar expression profiles of Msi-1 were observed at both mRNA and protein levels. In both the small intestine and the stomach, the transient expression of Msi-1 during metamorphosis spatio-temporally correlated well with active proliferation of the progenitor cells including stem cells of the adult epithelium but did not with apoptosis of the larval epithelium. As the adult progenitor cells differentiated into organ-specific epithelial cells after active proliferation, Msi-1 expression was rapidly downregulated. Therefore, Msi-1 is useful to identify the adult progenitor cells that actively proliferate before final differentiation in the amphibian gastrointestine. Furthermore, our culture experiments have shown that thyroid hormone (TH) organ-autonomously induces Msi-1 expression only in the adult progenitor cells of the *X. laevis* intestine in vitro as in vivo. However, TH could not induce Msi-1 expression in the intestinal epithelium separated from the connective tissue, where the adult epithelium never developed. These results suggest that Msi-1 expression is upregulated by TH in the adult progenitor cells under the control of the connective tissue and plays important roles in their maintenance and/or active proliferation during amphibian gastrointestinal remodeling.

Key words: Stem cells, Musashi-1, Thyroid hormone, Gastrointestinal remodeling, *Xenopus laevis*

Introduction

Amphibian metamorphosis is triggered by a single hormone, thyroid hormone (TH) (Dodd and Dodd, 1977; Kikuyama et al., 1993), and offers us a unique model system for the study of organ remodeling (Shi, 1999). In particular, to adapt to terrestrial carnivorous life, the amphibian gastrointestine dramatically undergoes remodeling from larval to adult form during a short period. At the cellular level, the primary (larval) epithelium undergoes apoptosis (Ishizuya-Oka and Ueda, 1996), whereas a small number of undifferentiated cells appear, replace the larval epithelium by active proliferation, and newly form the secondary (adult) epithelium (Hourdry and Dauca, 1977; Shi and Ishizuya-Oka, 1996). In the intestine, the adult epithelium acquires the cell renewal system along the trough-crest axis of newly formed folds (McAvoy and Dixon, 1977; Shi and Ishizuya-Oka, 1996) analogous to the mammalian crypt-villus axis (Cheng and Bjerknes, 1985; Madara and Trier, 1994), and finally differentiates into major absorptive epithelial cells expressing intestinal fatty acid-binding protein (IFABP) (Shi and Hayes, 1994; Ishizuya-Oka et al., 1997), goblet cells and endocrine cells (McAvoy and Dixon, 1978). Meanwhile, in the stomach, the adult epithelium acquires the cell renewal system where proliferating cells are localized in the neck region of glands (Oinuma et al., 1992) similar to that of the mammalian gastric glands (Lee and Leblond, 1985; Nomura et al., 1998), and finally differentiates into the surface mucous epithelium and the glandular epithelium, which consists of major glandular cells expressing pepsinogen (Pg) (Inokuchi et al., 1995; Ishizuya-Oka et al., 1998), mucous neck cells, and endocrine cells (Holmberg et al., 2001). Therefore, it is suggested that progenitor cells of the adult epithelium that appear as undifferentiated cells during metamorphosis in these organs include multipotent stem cells analogous to those in the mammalian gastrointestine. It is interesting from the standpoint of cell biology how the adult progenitor cells appear and form the mammalian-like epithelium. However, the progenitor cells of the adult gastrointestinal epithelium have thus far been only identified as morphologically undifferentiated cells stained strongly with pyronin Y (Ishizuya-Oka and Ueda, 1996). The lack of biochemical markers has made it difficult to

characterize the adult progenitor cells and has retarded the study of their origin and the mechanisms controlling their behavior.

Musashi-1 (Msi-1), an RNA-binding protein, was initially reported in the sensory organ of *Drosophila* (Nakamura et al., 1994) and has been shown to serve as a marker for proliferative neural precursor cells including stem cells in the central nervous system (CNS) (Sakakibara et al., 1996; Sakakibara and Okano, 1997). Msi-1 expression in neural precursor cells is evolutionally conserved in different species of vertebrates such as humans, mice and *Xenopus laevis* (Kaneko et al., 2000). Although its precise mechanisms have not yet been clarified, Msi-1 is supposed to be involved in the early asymmetric divisions that generate differentiated cells from neural stem cells (Okano, 1995). Interestingly, Msi-1 is also expressed in the murine intestine other than the neural tissues (Sakakibara et al., 1996). Moreover, it has been shown recently that Msi-1 is preferentially expressed in the predicted stem cell region of murine intestinal crypts, suggesting that Msi-1 may be a natural marker for intestinal stem cells and their immediate descendants (Booth and Potten, 2000; Potten et al., 2003). These recent reports led us to study the expression of Msi-1 during amphibian gastrointestinal remodeling.

In the present study, to clarify whether the adult progenitor cells in the amphibian gastrointestine express Msi-1 as in the mammalian intestine, we examined Msi-1 expression in the *X. laevis* small intestine and the stomach during metamorphosis at mRNA and protein levels. We show that expression profiles of Msi-1 coincide well with active proliferation of the adult progenitor cells in both organs, suggesting that Msi-1 serves as a marker for the stem cells common to the amphibian and mammalian intestines. Moreover, we demonstrate that cell-specific Msi-1 expression can be reproduced in vitro by the inductive action of TH in the presence of the connective tissue but not in its absence.

Materials and Methods

Tissue preparation

Tadpoles of the South African clawed frog (*X. laevis*) were purchased from a commercial source and staged according to Nieuwkoop and Faber (Nieuwkoop and Faber, 1967).

RNA isolation and reverse transcription-polymerase chain reaction (RT-PCR) analysis

Tissue fragments were isolated from the small intestine and the stomach of tadpoles at various stages, and of stage 57 tadpoles treated with or without 5 nM 3, 5, 3′-L-triiodo-thyronine (T_3). Total RNA was purified from these organs using Trizol reagent (Gibco-BRL, Grand Island, NY). RNAs were prepared from a mixture of more than three tadpoles at each stage. For each reaction, 1 μg RNA was reverse transcribed to oligo(dT)-primed first-strand cDNA by using a cDNA synthesis kit (Amersham Pharmacia Biotech, Little Chalfont, UK), and the resulting cDNA was subjected to 30 cycles of PCR with Msi-1-specific primers (5′-ATGGAGACAGAAGCGCCCCAGCC-CGGACTG-3′ and 5′-TCAGTGGTAGCCGTTGGTGAAAGCAG-3′) (Kaneko et al., 2000) and to 25 cycles with EF-1α-specific primers (5′-CCTGAATCACCCAGGCCAGATTGGTG-3′ and 5′-GAGG-GTAGTCTGAGAAGCTCTCCACG-3′) (Suzuki et al., 1993). The PCR products (5 μl) were electrophoresed through a 2% agarose gel and visualized by ethidium bromide staining.

Organ culture

Tissue fragments were isolated from the anterior part of the small intestine at stage 57 and were slit open lengthwise with fine forceps. Some fragments were treated with dispase (1000 units/ml; Godo, Tokyo, Japan), and their epithelial components were isolated and put on a growth factor-reduced matrigel (Becton Dickinson, Bedford, MA). They were then cultured as described previously (Ishizuya-Oka and Shimozawa, 1991). Briefly, they were placed on membrane filters (type HAWP; Millipore, Bedford, MA) on stainless steel grids and were cultured in 60% Leibovitz-15 medium supplemented with 100 IU/ml of penicillin, 100 μg/ml of streptomycin (Gibco-BRL), and 10% charcoal-treated fetal bovine serum (Gibco-BRL). To induce metamorphosis, T_3, insulin and hydrocortisone (Sigma) were added to the medium at 10 nM, 5 μg/ml and 0.5 μg/ml, respectively. The culture medium was changed every other day for 7 days at 26°C.

In situ hybridization

A cDNA fragment of nucleotides (nt) 74-1117 was amplified by PCR with the forward primer (5′-ATGGAGACAGAAGCGCCCCAG-CCCGGACTG-3′; nt 74-103), the reverse primer (5′-TCAGT-GGTAGCCGTTGGTGAAAGCAG; nt 1117-1092) and the template nrp1-pSP36T, containing *Xenopus* Msi-1 full-length cDNA. The cDNA fragment was subcloned into pCRII vector with TOPO TA cloning kit (Invitrogen, Carlsbad, CA). Procedures for in situ hybridization were the same as those described previously (Ishizuya-Oka et al., 1994). In brief, digoxigenin (DIG)-11-UTP-labeled antisense and sense probes were prepared with DIG RNA-labeling kit (Roche Diagnostics, Mannheim, Germany) according to the manufacturer's protocol. Tissue fragments were fixed with 4% paraformaldehyde in phosphate-buffered saline (pH 7.4) at 4°C for 4 hours, frozen on dry ice, and cut at 7 μm. Sections were treated with 0.2 N HCl, digested with 1 μg/ml proteinase K (Wako, Osaka, Japan), and then fixed again with 4% paraformaldehyde. Hybridization buffer containing DIG-labeled antisense RNA probe (200 ng/ml) was applied to the pretreated sections. After hybridization at 40°C for 18 hours, the sections were treated with 20 μg/ml RNase A (Wako) at 37°C for 30 minutes to remove excess unhybridized probes. They were then washed, processed for immunological detection of the hybridized DIG probes according to the manufacturer's instructions (DIG-probe Detection Kit, Roche Diagnostics), and examined microscopically. As controls, some sections were hybridized with DIG-labeled sense RNA probe (200 ng/ml).

Immunohistochemistry for IFABP, Pg and PCNA

Tissue fragments and cultured explants were fixed with 95% ethanol at 4°C for 4 hours, embedded in paraffin and cut at 5 μm. The sections were incubated at 4°C overnight with the rabbit anti-mouse Msi-1 polyclonal antibody (diluted 1:100) (Sakakibara et al., 1996) or with the rat anti-mouse Msi-1 monoclonal antibody (diluted 1:100), which has been shown to recognize the amino acid sequences highly conserved between *Xenopus* and mouse (Kaneko et al., 2000). They were then incubated with the biotinylated secondary antibody, followed by incubation with avidin-conjugated horseradish peroxidase (HRP) (Vector Labs, Burlingame, CA). HRP reactions were developed using 0.02% 3, 3′-diamino-benzidine-4HCl (DAB) and 0.006% H_2O_2. Although the immunostaining with the monoclonal antibody was somewhat weaker than that with the polyclonal antibody, their expression profiles were spatio-temporally consistent (data not shown).

To distinguish between the adult progenitor cells and the remaining larval cells during stages 60-62, some sections close to the sections used for Msi-1 immunohistochemistry were stained with methyl green-pyronin Y (Muto, Tokyo, Japan) for 5 minutes. The adult progenitor cells were stained intensely red because of their RNA-rich cytoplasm, whereas the larval epithelial cells undergoing apoptosis

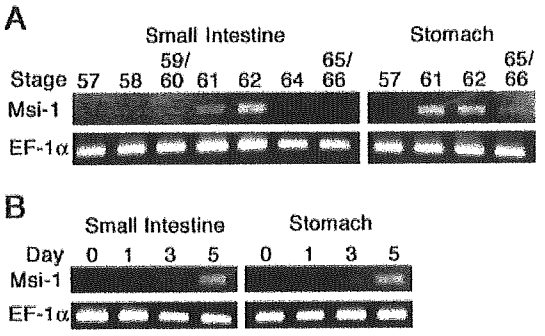

Fig. 1. Expression of Msi-1 mRNA in *X. laevis* intestine and stomach analyzed by RT-PCR. (A) Developmental changes during normal metamorphosis. Msi-1 mRNA is expressed transiently around stages 61-62. (B) Expression of Msi-1 mRNA in stage 57 tadpoles treated with 5 nM TH in vivo. Msi-1 mRNA becomes detectable around day 5. The two products of Msi-1 mRNA with different sizes are produced by alternative splicing (Kaneko et al., 2000). The products of EF-1α mRNA serve as a control.

were stained much weaker (Ishizuya-Oka and Ueda, 1996). In addition, other sections were incubated at room temperature for 1 hour with the following antibodies: the mouse anti-PCNA monoclonal antibody (diluted 1:100; Novacastra, Newcastle, UK) for proliferating cells; the rabbit anti-*Xenopus* IFABP antibody (diluted 1:1000) (generous gift of Dr Y.-B. Shi) (Ishizuya-Oka et al., 1997) for differentiated intestinal absorptive cells; and the rabbit anti-bullfrog Pg antibody (diluted 1:10,000) (generous gift of Dr T. Inokuchi) (Ishizuya-Oka et al., 1998) for differentiated glandular cells. They were then visualized by sequential incubation with streptavidin-biotin-peroxidase complex (Nichirei, Tokyo, Japan) and DAB/H_2O_2 as described above. There was no positive staining when the same concentration of pre-immune or normal serum was applied for each antiserum as the specificity control (not shown). At least three specimens were examined for each developmental stage or culture day.

Finally, to examine the relationship between Msi-1 immunoreactivity and cell proliferation more directly, some sections were double immunostained with a mixture containing the rabbit anti-Msi-1 antibody and the mouse anti-PCNA antibody at 4°C overnight. They were then incubated with a mixture containing Alexa Fluor488-conjugated anti-rabbit IgG (1:500; Molecular Probes, Eugene, OR) and Alexa Fluor568-conjugated anti-mouse IgG (1:500; Molecular Probes) and observed by fluorescence microscopy.

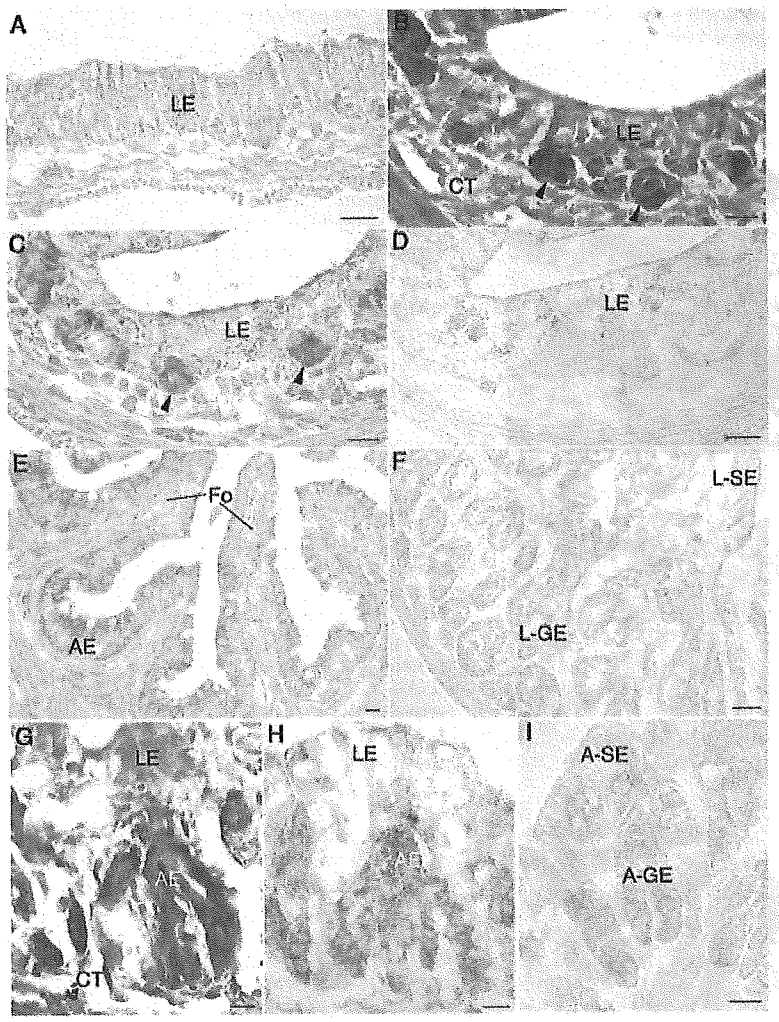

Results

Expression of Msi-1 mRNA during normal and TH-induced metamorphosis

To clarify whether Msi-1 mRNA was truly expressed in the *X. laevis* intestine, its developmental expression was analyzed by RT-PCR. The level of Msi-1 mRNA began to increase at the onset of metamorphic climax (around stage 61) and peaked around stage 62 (Fig. 1A), when the circulating level of TH peaks (Leloup and Buscaglia, 1977). Subsequently, the level of Msi-1 mRNA decreased towards the end of metamorphosis. Similarly, in the stomach, the expression of Msi-1 mRNA was transiently upregulated around stages 61-62. In addition, to clarify whether TH upregulates Msi-1 mRNA expression in vivo,

Fig. 2. Developmental expression of Msi-1 mRNA during metamorphosis. Cross-sections of the small intestine (A-E) and the stomach (F-I) were hybridized with the antisense (A,C,E,F,H,I) and sense (D) probes and stained with methyl green-pyronin Y (B,G). (A) Stage 58. No specific signals are detectable. (B-D) Stage 61. Adult progenitor cells (arrowheads) between the larval epithelium (LE) and the connective tissue (CT) are positive. No signals are detectable in the control section (D). (E) Stage 65. The adult epithelium (AE) is almost negative except for very weak signals in the trough of intestinal folds (Fo). (F) Stage 58. No specific signals are detectable in the larval surface (L-SE) and glandular epithelia (L-GE). (G,H) Stage 61. Signals are localized in adult progenitor cells. (I) Stage 65. The adult surface (A-SE) and glandular epithelia (A-GE) are almost negative. Weak signals in the neck region of glands are nonspecific. Bars, 20 μm.

stage 57 tadpoles were treated with TH. Msi-1 mRNA was precociously detected in the both organs after 5 days of TH treatment (Fig. 1B), when metamorphic changes occur most dramatically (Shi and Ishizuya-Oka, 2001).

Msi-1 mRNA expression is specific for progenitor cells of adult epithelium

To identify which type of cells express Msi-1 mRNA, we performed in situ hybridization analysis. Consistent with the RT-PCR data described above (Fig. 1A), Msi-1 mRNA was neither detected in the intestine (Fig. 2A) nor the stomach (Fig. 2F) throughout pre- and prometamorphosis. In the intestine, around the onset of metamorphic climax (stages 60-61), when progenitor cells of the adult epithelium were identified as islets stained strongly with pyronin-Y (Fig. 2B), Msi-1 mRNA became detectable only in these adult progenitor cells (Fig. 2C). By contrast, all the control hybridizations with the sense RNA probe gave only background levels of signals (Fig. 2D). Thereafter, as morphogenesis of intestinal folds proceeded, the level of Msi-1 mRNA rapidly decreased from the crest to trough of the folds (Fig. 2E). By the end of metamorphosis (stage 66), Msi-1 mRNA became hardly detectable, if any. Similarly, in the stomach, Msi-1 mRNA was transiently expressed only in pyronin-Y-positive adult progenitor cells during stages 60-61 (Fig. 2G,H). Then, as the adult progenitor cells differentiated into the surface and glandular epithelia, the level of Msi-1 mRNA rapidly decreased. By stage 66, Msi-1 mRNA became hardly detectable, if any, except for nonspecific staining in the neck region of glands (Fig. 2I).

Transient expression of Msi-1 protein correlates with active proliferation of adult progenitor cells

To investigate the relationship between Msi-1 expression and development of the adult epithelium more precisely, we analyzed the expression profile of Msi-1 proteins by immunohistochemistry.

Small intestine

Throughout pre- and prometamorphosis, the larval epithelium remained simple columnar and negative for Msi-1 (Fig. 3A). At stage 60, when progenitor cells of the adult epithelium were first identified as pyronin-Y-positive small islets (Fig. 3B), Msi-1 immunoreactivity became weakly detectable only in these islets (Fig. 3C). Then, at stage 61, when the adult progenitor cells rapidly replaced the larval epithelium (Fig. 3D) by active proliferation (Fig. 3E), almost all of the progenitor cells were positive for Msi-1 (Fig. 3F). Double immunofluorescence labeling with Msi-1 and PCNA antibodies indicated that Msi-1-positive cells have a high activity of cell proliferation (Fig. 4A). By contrast, the degenerating larval epithelial cells remained negative (Fig. 3D,F). After the completion of larval-to-adult epithelial cell replacement (stage 63) (Fig. 3G), Msi-1 immunoreactivity rapidly decreased and became weakly detectable only in the trough of newly formed folds (Fig. 3H), where proliferating cells became localized (Fig. 3I). By contrast, the immunoreactivity of IFABP, a marker for differentiated absorptive cells, increased from the crest to trough of the folds (Fig. 3J). At the end of metamorphosis, Msi-1 expression was hardly detectable, if any.

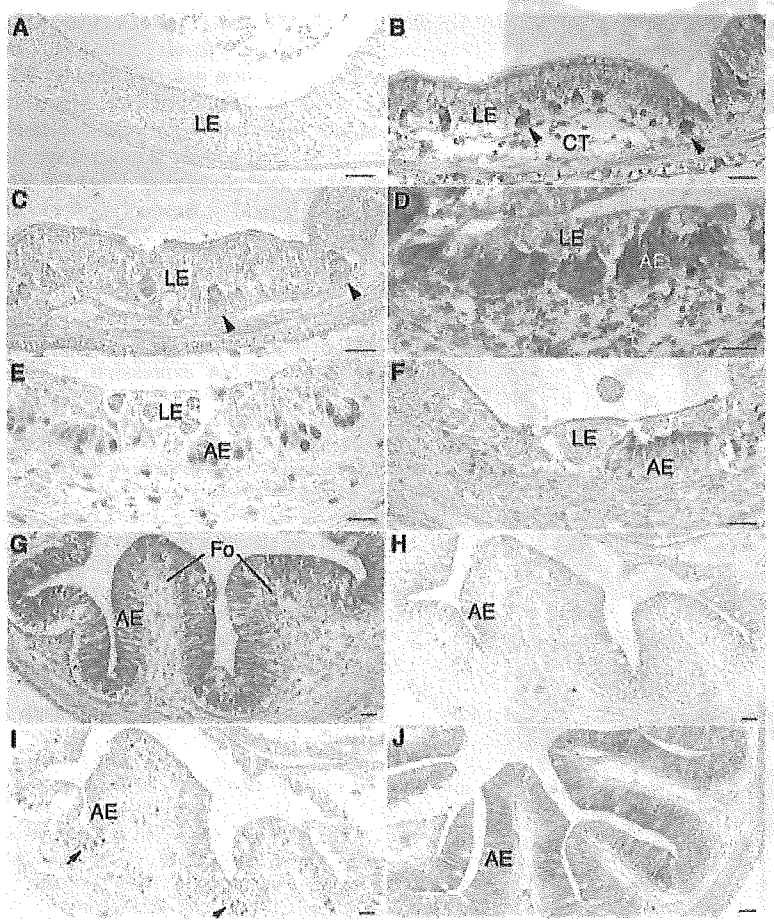

Fig. 3. Msi-1 expression correlates spatio-temporally with adult progenitor cells during intestinal remodeling. Cross-sections were immunostained with Msi-1 (A,C,F,H), PCNA (E,I) and IFABP (J) antibodies and stained with methyl green-pyronin Y (B,D,G). (A) Stage 57. The larval epithelium (LE) is negative for Msi-1. (B,C) Stage 60. Progenitor cells of the adult epithelium between the larval epithelium and the connective tissue (CT) are weakly positive for Msi-1 (arrowheads). (D-F) Stage 61. The adult epithelium (AE), where PCNA-positive cells are localized, is positive for Msi-1. The degenerating larval epithelium remains negative. (G-J) Stage 63. The adult epithelium completely replaces the larval one. Msi-1-immunoreactivity is weakly detectable only in the trough of newly formed folds (Fo), where PCNA-positive cells are localized (I; arrows). IFABP immunoreactivity increases in intensity from the crest to the trough of the folds. Bars, 20 μm.

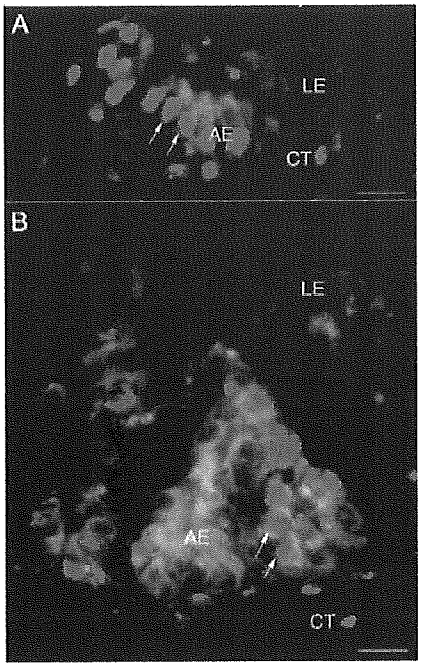

Fig. 4. Coexpression of Msi-1 and PCNA in the intestine (A) and the stomach (B) at stage 61. Msi-1 (green) and PCNA (red) double-positive cells (arrows) are localized in the adult epithelium (AE) but not in the larval epithelium (LE). CT, connective tissue. Bars, 20 μm.

Stomach

As in the intestine, Msi-1 became detectable at stage 60 only in the adult progenitor cells, which appeared in the basal region of larval glands (Fig. 5A-C) and were actively proliferating (Fig. 5D). Then, at stage 61, the proliferating adult progenitor cells rapidly replaced the degenerating larval epithelium (Fig. 5E,F). Almost all of the adult progenitor cells were strongly positive for Msi-1, whereas all of the larval epithelial cells remained negative (Fig. 5G). Msi-1-positive cells at this stage have a high activity of cell proliferation (Fig. 4B) just like in the intestine. After stage 62, when the adult epithelium completely replaced the larval epithelium and began to differentiate into the surface and glandular epithelia (Fig. 5H) expressing Pg, a marker for differentiated glands (Fig. 5I), Msi-1 expression rapidly decreased (Fig. 5J). Towards the end of metamorphosis, Msi-1 immunoreactivity became hardly detectable except for a very weak one in the neck region of adult glands (Fig. 5L), where proliferating cells were localized (Fig. 5K).

TH organ-autonomously upregulates Msi-1 expression in vitro

To clarify whether TH upregulates Msi-1 expression in vitro, we cultured larval intestines isolated from stage 57 tadpoles in the presence or absence of TH. Around day 5 in the presence of TH, progenitor cells of the adult epithelium were identified as pyronin-Y-positive islets (Fig. 6A) that were actively proliferating (Fig. 6B). Although the intensity of Msi-1 immunoreactivity was lower than in vivo, it was localized in the adult progenitor cells but not in the remaining larval cells as in vivo (Fig. 6C). Towards day 7, when the adult epithelium differentiated into the absorptive epithelium expressing IFABP (Fig. 6E), Msi-1-immunoreactive cells became undetectable again (Fig. 6F). By contrast, in the absence of TH, the differentiated larval epithelium remained negative for Msi-1 throughout the cultivation (Fig. 6D).

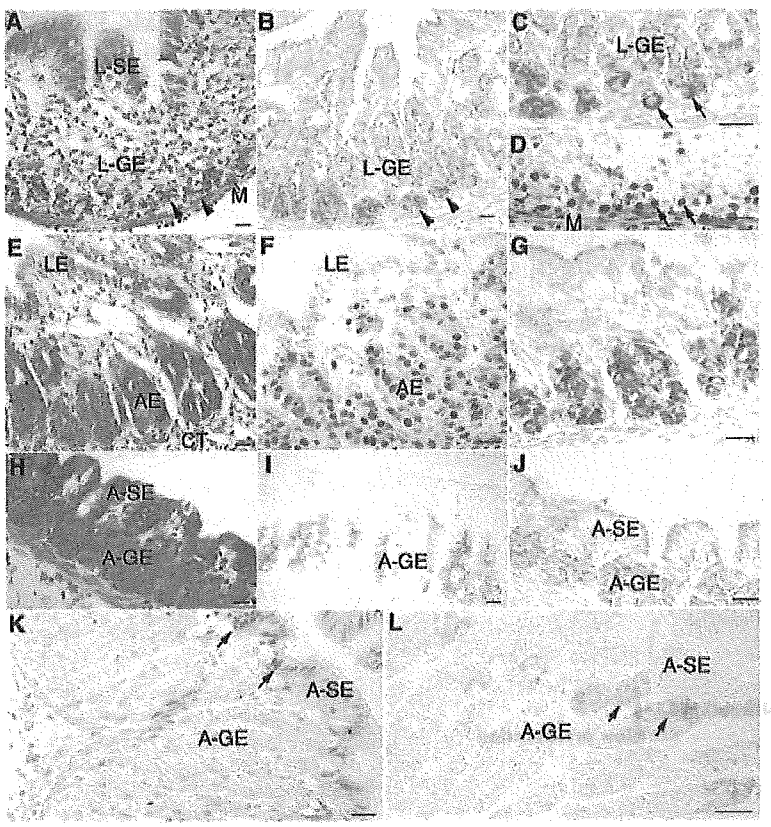

Fig. 5. Msi-1 expression correlates with adult progenitor cells during gastric remodeling. Cross-sections were immunostained with Msi-1 (B,C,G,J,L), PCNA (D,F,K) and Pg (I) antibodies, and stained with methyl green-pyronin Y (A,E,H). (A-D) Stage 60. Progenitor cells of the adult epithelium appear in the basal region of larval glands (L-GE) and are positive for Msi-1 (A,B; arrowheads). Msi-1 immunoreactivity is localized in the cytoplasm of these cells, which are actively proliferating (C,D; arrows). L-SE, larval surface epithelium; M, muscles. (E-G) Stage 61. The adult epithelium (AE) is positive for Msi-1, whereas the larval epithelium (LE) remains negative. CT, connective tissue. (H-J) Stage 62. The adult epithelium completely replaces the larval one and begins to differentiate into the surface (A-SE) and glandular epithelia (A-GE) expressing Pg (I). Msi-1 immunoreactivity becomes weak. (K,L) Stage 66. Msi-1 immunoreactivity is weakly detectable only in the neck region of glands, where proliferating cells are localized (arrows). Bars, 20 μm.

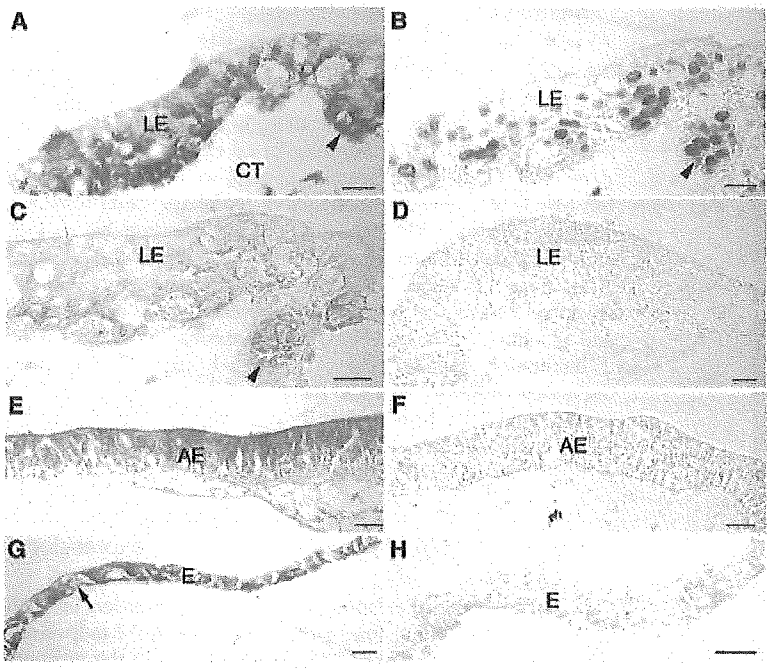

Fig. 6. TH upregulates Msi-1 expression in adult progenitor cells of isolated intestines in vitro in the presence of the connective tissue (A-F) but not in its absence (G,H). Cross-sections were immunostained with Msi-1 (C,D,F,H), PCNA (B) and IFABP (E) antibodies and stained with methyl green-pyronin Y (A,G). (A-C) Day 5 in the presence of TH. Adult progenitor cells, which are identified as islets between the larval epithelium (LE) and the connective tissue (CT), are actively proliferating and positive for Msi-1 (arrowhead). (D) Day 5 in the absence of TH. The larval epithelium remains negative. (E,F) Day 7 in the presence of TH. The adult epithelium is differentiated into the absorptive epithelium expressing IFABP and negative for Msi-1. (G,H) Day 5 in the epithelium (E) alone in the presence of TH. Some cells of the simple epithelium are negative for pyronin-Y staining (arrow), whereas the others are positive at various intensities. The epithelium remains negative for Msi-1. Bars, 20 μm.

Furthermore, to determine whether the connective tissue surrounding the epithelium is involved in TH upregulation of Msi-1 expression, we separated the epithelium from the connective tissue and cultured it alone in the presence of TH. Around day 5, some epithelial cells became negative for pyronin-Y staining, just like degenerating larval cells in the presence of the connective tissue (Fig. 6G). However, the adult progenitor cells could be hardly distinguished by pyronin-Y staining because the other cells were stained at various intensities. In addition, the epithelial cells remained as a single layer and did not form islet structures. Thereafter, the epithelium gradually decreased in cell number and never differentiated into the adult absorptive epithelium expressing IFABP. In this condition, no Msi-1-immunoreactive cells could be detected throughout the cultivation (Fig. 6H).

Discussion

Msi-1 serves as a common stem cell marker in both amphibian and mammalian intestines

In the present study, the transient expression of Msi-1 coincides well with active proliferation of progenitor cells of the adult epithelium in the intestine, as schematically summarized in Fig. 7. Similar correlation was also observed in the stomach. Although previous studies reported some TH response genes whose expression is epithelial specific in the amphibian intestine (Shi and Ishizuya-Oka, 1996; Ishizuya-Oka et al., 2001), Msi-1 is the only one that is specifically expressed in adult progenitor cells that are actively proliferating, but not in differentiated adult epithelial cells nor larval cells destined to undergo apoptosis. As for other markers, pyronin-Y strongly stains the adult progenitor cells. However, it also stains the larval epithelium before apoptosis, as well as the differentiated

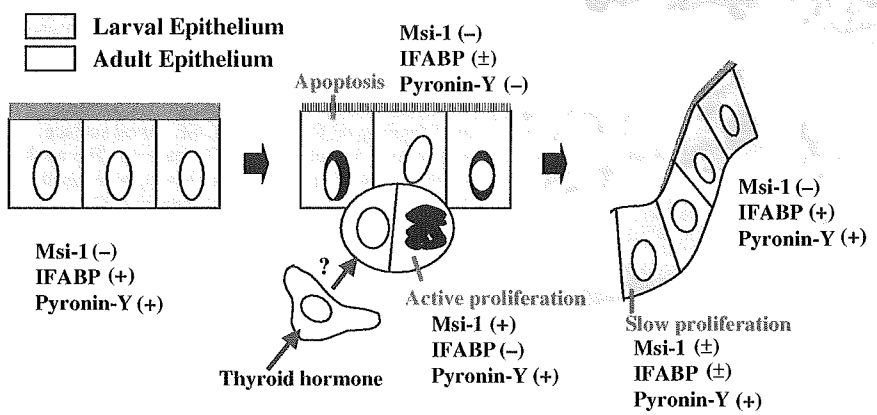

Fig. 7. Msi-1 expression during larval-to-adult epithelial transformation in the *X. laevis* intestine. Msi-1 expression is associated with active proliferation of adult progenitor cells and is complementary to IFABP expression.

adult epithelium, and other tissues (Ishizuya-Oka and Ueda, 1996), because the RNA-rich cytoplasm is stained with pyronin-Y regardless of cell types (Schulte et al., 1992). Similarly, PCNA immunostains not only the adult progenitor cells but also the larval epithelium and other tissues at various frequencies. Thus, Msi-1 is the first reliable marker for the adult progenitor cells including stem cells in the amphibian gastrointestine. It is noteworthy that Msi-1 expression is also expressed in the mammalian intestine (Sakakibara et al., 1996), where putative stem cells and at least the next two generations are positive for Msi-1 (Potten et al., 2003). Although Msi-1 expression became hardly detectable towards the end of metamorphosis, possibly due to a low immunoreactive sensitivity in this study, Msi-1 expression could be detectable in the region where proliferating cells were localized in both the intestine and the stomach, that is, in the trough of intestinal folds corresponding to the mammalian crypt (Cheng and Bjerknes, 1985; Potten et al., 1997) or in the neck region of gastric glands similar to that of mammalian glands (Lee and Leblond, 1985). These results indicate that the adult progenitor cells during amphibian metamorphosis include stem cells analogous to the mammalian ones, and molecular mechanisms underlying the control of these stem cells are conserved across the amphibian and mammalian gastrointestines.

Recently, in the mammalian CNS, it has been shown that Msi-1 protein binds to (G/A) UnAGU sequences in the 3′-untranslated region (3′-UTR) of Numb mRNA and represses the expression of Numb protein (Imai et al., 2001), which is a membrane-associated antagonist of Notch signaling (Wakamatsu et al., 1999). Meanwhile, in the mammalian intestine, Notch signaling has been suggested to be involved in the determination and/or maintenance of stem cells (van den Brink et al., 2001). Taken together, one possible role of Msi-1 is to maintain the adult progenitor cells through activation of Notch signaling. Alternatively, Msi-1 may bind to (G/A) UnAGU sequences of other target genes that activate proliferation of the adult progenitor cells. The nature of these target genes awaits further investigation.

TH upregulates Msi-1 expression in adult progenitor cells in vitro as in vivo

In the mammalian intestine, it has been reported that Msi-1 expression is upregulated during development of adenomas and during regeneration after irradiation (Potten et al., 2003). However, it remains unknown which molecules upregulate Msi-1 expression. In the present study, the upregulation of Msi-1 expression coincides temporally with the peak of circulating TH level during *X. laevis* metamorphosis (Leloup and Buscaglia, 1977). More importantly, our culture study has shown that TH upregulates organ-autonomously Msi-1 expression in the larval intestine. This means that Msi-1 gene is a TH response gene, as recently reported in the developing rat brain (Cuadrado et al., 2002). Furthermore, we have shown that Msi-1 expression in vitro is closely associated with adult progenitor cells that are actively proliferating just like in vivo. This reinforces our proposal that TH-induced Msi-1 is involved in the maintenance and/or active proliferation of adult progenitor cells.

Until now, little is known about the origin of the adult progenitor cells in the amphibian gastrointestine. In the intestinal epithelium before metamorphosis, no undifferentiated cells can be morphologically identified (Marshall and Dixon, 1978). In agreement with this, Msi-1 expression was not detected in the intestinal epithelium before metamorphosis in the present study. This implies that at least partially differentiated cells can give rise to progenitor and/or stem cells during amphibian metamorphosis. Similar cases have recently been reported in the mammalian tissues such as committed oligodendrocyte precursor cells that become multipotent stem cells (Kondo and Raff, 2000) and multinucleated myotubes that give rise to mononucleated proliferative myoblasts (Odelberg et al., 2000). Although the important roles of microenvironments known as 'niche' in the control of stem cells are generally recognized (Potten et al., 1997; Blau et al., 2001; Mills and Gordon, 2001; Spradling et al., 2001), far less is known about microenvironmental factors that play key roles in reversing the differentiated state (i.e. de-differentiation into stem cells). In this study, we have shown that the adult progenitor cells expressing Msi-1 could be detected after 5 days of TH treatment in vitro in the connective tissue but not in its absence. This predicts that genes whose expression is upregulated by TH in the connective tissue within 5 days play important roles in the de-differentiation. To identify such factors, we recently isolated genes whose expression is upregulated by TH in the connective tissue by subtractive differential screening (Shimizu et al., 2002). It is worth functionally analyzing these genes as well as other TH response genes previously isolated from the *X. laevis* intestine (Shi and Brown, 1993; Amano and Yoshizato, 1998).

In conclusion, Msi-1 is useful as a marker for adult progenitor cells including stem cells in the amphibian gastrointestinal epithelium like in the mammalian intestinal epithelium. Amphibian gastrointestinal remodeling, where TH can induce stem cells expressing Msi-1 followed by a new epithelial formation, should provide a unique model system to clarify microenvironmental factors playing key roles in the control of stem cells.

We express our deep gratitude to Y.-B. Shi (National Institutes Health) and T. Inokuchi (Utsunomiya University) for their generous gifts of antibodies. This work was supported in part by the MEXT Grants-in-Aid for Scientific Research (C) and Research Grant of Seki Minato Foundation (to A.I.-O.).

References

Amano, T. and Yoshizato, K. (1998). Isolation of genes involved in intestinal remodeling during anuran metamorphosis. *Wound Rep. Reg.* **6**, 302-313.

Blau, H. M., Brazelton, T. R. and Weimann, J. M. (2001). The evolving concept of a stem cell: entity or function? *Cell* **105**, 829-841.

Booth, C. and Potten, C. S. (2000). Gut instincts: thoughts on intestinal epithelial stem cells. *J. Clin. Invest.* **105**, 1493-1499.

Cheng, H. and Bjerknes, M. (1985). Whole population cell kinetics and postnatal development of the mouse intestinal epithelium. *Anat. Rec.* **211**, 420-426.

Cuadrado, A., Garcia-Fernandez, L. F., Imai, T., Okano, H. and Munoz, A. (2002). Regulation of *tau* RNA maturation by thyroid hormone is mediated by the neural RNA-binding protein Musashi-1. *Mol. Cell. Neurosci.* **20**, 198-210.

Dodd, M. H. I. and Dodd, J. M. (1977). The biology of metamorphosis. In *Physiology of Amphibia*, Vol 3 (ed. B. Lofts), pp. 467-599. New York: Academic Press.

Holmberg, A., Hagg, U., Fritsche, R. and Holmgren, S. (2001). Occurrence of neurotrophin receptors and transmitters in the developing *Xenopus* gut. *Cell Tissue Res.* **306**, 35-47.

Hourdry, J. and Dauca, M. (1977). Cytological and cytochemical changes in the intestinal epithelium during anuran metamorphosis. *Int. Rev. Cytol. [Suppl.]* **5**, 337-385.

Imai, T., Tokunaga, A., Yoshida, T., Hashimoto, M., Mikoshiba, K., Weinmaster, G., Nakafuku, M. and Okano, H. (2001). The neural RNA-binding protein Musashi1 translationally regulates mammalian numb gene expression by interacting with its mRNA. *Mol. Cell. Biol.* **21**, 3888-3900.

Inokuchi, T., Kobayashi, K. and Horiuchi, S. (1995). Isolation of pepsinogen A from gastric mucosa of bullfrog, *Rana catesbeiana*. *Comp. Biochem. Physiol.* **111**, 111-117.

Ishizuya-Oka, A. and Shimozawa, A. (1991). Induction of metamorphosis by thyroid hormone in anuran small intestine cultured organotypically in vitro. *In Vitro Cell. Dev. Biol.* **27A**, 853-857.

Ishizuya-Oka, A. and Ueda, S. (1996). Apoptosis and cell proliferation in the *Xenopus* small intestine during metamorphosis. *Cell Tissue Res.* **286**, 467-476.

Ishizuya-Oka, A., Shimozawa, A., Takeda, H. and Shi, Y.-B. (1994). Cell-specific and spatio-temporal expression of intestinal fatty acid-binding protein gene during amphibian metamorphosis. *Roux's Arch. Dev. Biol.* **204**, 150-155.

Ishizuya-Oka, A., Ueda, S., Damjanovski, S., Li, Q., Liang, V. C.-T. and Shi, Y.-B. (1997). Anteroposterior gradient of epithelial transformation during amphibian intestinal remodeling: immunohistochemical detection of intestinal fatty acid-binding protein. *Dev. Biol.* **192**, 149-161.

Ishizuya-Oka, A., Inokuchi, T. and Ueda, S. (1998). Thyroid hormone-induced apoptosis of larval cells and differentiation of pepsinogen-producing cells in the stomach of *Xenopus laevis* in vitro. *Differentiation* **63**, 59-68.

Ishizuya-Oka, A., Ueda, S., Inokuchi, T., Amano, T., Damjanovski, S., Stolow, M. and Shi, Y.-B. (2001). Thyroid hormone-induced expression of Sonic hedgehog correlates with adult epithelial development during remodeling of the *Xenopus* stomach and intestine. *Differentiation* **69**, 27-37.

Kaneko, Y., Sakakibara, S., Imai, T., Suzuki, A., Nakamura, Y., Sawamoto, K., Ogawa, Y., Toyama, Y., Miyata, T. and Okano, H. (2000). Musashi1: an evolutionally conserved marker for CNS progenitor cells including neural stem cells. *Dev. Neurosci.* **22**, 139-153.

Kikuyama, S., Kawamura, K., Tanaka, S. and Yamamoto, K. (1993). Aspects of amphibian metamorphosis: hormonal control. *Int. Rev. Cytol.* **145**, 105-148.

Kondo, T. and Raff, M. (2000). Oligodendrocyte precursor cells reprogrammed to become multipotential CNS stem cells. *Science* **289**, 1754-1757.

Lee, E. R. and Leblond, C. P. (1985). Dynamic histology of the antral epithelium in the mouse stomach: IV. Ultrastructural and renewal of gland cells. *Am. J. Anat.* **172**, 241-259.

Leloup, J. and Buscaglia, M. (1977). La triiodothyronine: hormone de la metamorphose des amphibiens. *C. R. Acad. Sci.* **284**, 2261-2263.

Madara, J. L. and Trier, J. S. (1994). Functional morphology of the mucosa of the small intestine. In *Physiology of the Gastrointestinal Tract*, 3rd edn. (ed. L. R. Johnson), pp. 1577-1622. New York: Raven Press

Marshall, J. A. and Dixon, K. E. (1978). Cell specialization in the epithelium of the small intestine of feeding *Xenopus laevis* tadpoles. *J. Anat.* **126**, 133-144.

McAvoy, J. W. and Dixon, K. E. (1977). Cell proliferation and renewal in the small intestinal epithelium of metamorphosing and adult *Xenopus laevis*. *J. Exp. Zool.* **202**, 129-138.

McAvoy, J. W. and Dixon, K. E. (1978). Cell specialization in the small intestinal epithelium of adult *Xenopus laevis*. *J. Anat.* **125**, 155-169.

Mills, J. C. and Gordon, J. I. (2001). The intestinal stem cell niche: there grows the neighborhood. *Proc. Natl. Acad. Sci. USA* **98**, 12334-12336.

Nakamura, M., Okano, H., Blendy, J. and Montell, C. (1994). Musashi, a neural RNA-binding protein required for *Drosophila* adult external sensory organ development. *Neuron* **13**, 67-81.

Nieuwkoop, P. D. and Faber, J. (1967). Normal Table of *Xenopus laevis* (Daudin). Amsterdam: North-Holland Pub.

Nomura, S., Esumi, H., Job, C. and Tan, S. S. (1998). Lineage and clonal development of gastric glands. *Dev. Biol.* **204**, 124-135.

Odelberg, S. J., Kollhoff, A. and Keating, M. T. (2000). Dedifferentiation of mammalian myotubes induced by msx-1. *Cell* **103**, 1099-1109.

Oinuma, T., Kawano, J. and Suganuma, T. (1992). Bromodeoxyuridine-immunohisto-chemistry on cellular differentiation and migration in the fundic gland of *Xenopus laevis* during development. *Cell Tissue Res.* **269**, 205-212.

Okano, H. (1995). Two major mechanisms regulating cell-fate decisions in the developing nervous system. *Dev. Growth Diff.* **37**, 619-629.

Potten, C. S., Booth, C. and Pritchard, D. M. (1997). The intestinal epithelial stem cell: the mucosal governor. *Int. J. Exp. Pathol.* **78**, 219-243.

Potten, C. S., Booth, C., Tudor, G. L., Booth, D., Brady, G., Hurley, P., Ashton, G., Clarke, R., Sakakibara, S. and Okano, H. (2003). Identification of a putative intestinal stem cell and early lineage marker; musashi-1. *Differentiation* **71**, 28-41.

Sakakibara, S. and Okano, H. (1997). Expression of neural RNA-binding proteins in the postnatal CNS: implications of their roles in neuronal and glial cell development. *J. Neurosci.* **17**, 8300-8312.

Sakakibara, S., Imai, T., Hamaguchi, K., Okabe, M., Aruga, J., Nakajima, K., Yasutomi, D., Nagata, T., Kurihara, Y., Uesugi, S. et al. (1996). Mouse-Musashi-1, a neural RNA-binding protein highly enriched in the mammalian CNS stem cell. *Dev. Biol.* **176**, 230-242.

Schulte, E. K. W., Lyon, H. O. and Hoyer, P. E. (1992). Simultaneous quantidication of DNA and RNA in tissue sections. A comparative analysis of the methyl green-pyronin technique with the gallovyanin chtomalum and Feukgen procedures. *Histochem. J.* **24**, 305-310.

Shi, Y.-B. (1999). Amphibian metamorphosis: from morphology to molecular biology. New York: Wiley-Liss Pub.

Shi, Y.-B. and Brown, D. D. (1993). The earliest changes in gene expression in tadpole intestine induced by thyroid hormone. *J. Biol. Chem.* **268**, 20312-20317.

Shi, Y.-B. and Hayes, W. P. (1994). Thyroid hormone-dependent regulation of the intestinal fatty acid-binding protein gene during amphibian metamorphosis. *Dev. Biol.* **161**, 48-58.

Shi, Y.-B. and Ishizuya-Oka, A. (1996). Biphasic intestinal development in amphibians: embryogenesis and remodeling during metamorphosis. *Curr. Top. Dev. Biol.* **32**, 205-235.

Shi, Y.-B. and Ishizuya-Oka, A. (2001). Thyroid hormone regulation of apoptotic tissue remodeling: implications from molecular analysis of amphibian metamorphosis. *Prog. Nucleic Acid Res. Mol. Biol.* **65**, 53-100.

Shimizu, K., Ishizuya-Oka, A., Amano, A., Yoshizato, K. and Ueda, S. (2002). Isolation of connective tissue-specific genes involved in *Xenopus* intestinal remodeling: thyroid hormone up-regulates Tolloid/BMP-1 expression. *Dev. Genes Evol.* **212**, 357-364.

Spradling, A., Drummond-Barbosa, D. and Kai, T. (2001). Stem cells find their niche. *Nature* **414**, 98-104.

Suzuki, A., Nishimatsu, S.-I., Murakami, K. and Ueno, N. (1993). Differential expression of *Xenopus* BMPs in early embryos and tissues. *Zool. Sci.* **10**, 175-178.

van den Brink, G. R., de Santa Barbara, P. and Roberts, D. J. (2001). Epithelial cell differentiation – a Mather of choice. *Science* **294**, 2115-2116.

Wakamatsu, Y., Maynard, T. M., Jones, S. U. and Weston, J. A. (1999). Numb localizes in the basal cortex of mitotic avian neuroepithelial cells and modulates neuronal differentiation by binding to Notch-1. *Neuron* **23**, 71-81.

Cytosol-endoplasmic reticulum interplay by Sec61α translocon in polyglutamine-mediated neurotoxicity in *Drosophila*

Hirotaka Kanuka*†, Erina Kuranaga*‡§, Tetsuo Hiratou*, Tatsushi Igaki*‡§, Bryce Nelson*, Hideyuki Okano¶‖, and Masayuki Miura*§**

*Laboratory for Cell Recovery Mechanisms, RIKEN Brain Science Institute, 2-1 Hirosawa, Wako, Saitama 351-0198, Japan; ‡Department of Cell Biology and Neuroscience, Osaka University Graduate School of Medicine, 2-2 Yamadaoka, Suita, Osaka 565-0871, Japan; ¶Department of Physiology, Keio University School of Medicine, 35 Shinanomachi, Shinjuku-ku, Tokyo 160-8582, Japan; ‖Core Research for Evolutional Science and Technology (CREST), Japan Science and Technology Corporation (JST), Saitama 332-0012, Japan; and §Department of Genetics, Graduate School of Pharmaceutical Sciences, University of Tokyo, 7-3-1 Hongo, Bunkyo-ku, Tokyo 113-0033, Japan

Communicated by Randy Schekman, University of California, Berkeley, CA, July 28, 2003 (received for review February 17, 2003)

Intracellular deposition of aggregated and ubiquitinated proteins is a prominent cytopathological feature of most neurodegenerative disorders frequently correlated with neural cell death. To elucidate mechanisms in neural cell death and degeneration, we characterized the *Drosophila* ortholog of Sec61α (DSec61α), a component of the translocon that is involved in both protein import and endoplasmic reticulum-associated degradation. Loss-of-function experiments for DSec61α revealed that the translocon contributes to expanded polyglutamine-mediated neuronal toxicity, likely resulting from proteasome inhibition and leading to accumulation of ubiquitinated proteins. Taken together, proteasome inhibition by expanded polyglutamine tracts may lead to the accumulation of toxic undegraded proteins normally transported by the Sec61α translocon.

In a wide variety of neurodegenerative diseases, unfolded polypeptides accumulate in cells, largely as insoluble inclusions, and appear to play a critical role in disease pathogenesis such as amyotrophic lateral sclerosis, Alzheimer's disease, and Parkinson's disease, and several hereditary diseases caused by the expansion of polyglutamine tracts (e.g., Huntington's disease or the spinocerebeller ataxias). In all of these neurodegenerative diseases, the pathology and eventual death of specific neuronal populations occurs as a result of the accumulation of distinctly abnormal polypeptides (1). Many observations suggest that these various types of inclusions arise through common mechanisms that elicit similar host responses. For example, they all contain components of the ubiquitin-proteasome degradative pathway as well as molecular chaperones, representing the two main systems that protect eukaryotic cells against the buildup of unfolded polypeptides (1). In fact, the transient expression of an expanded polyglutamine tract causes nearly partial inhibition of the ubiquitin-proteasome system in cell culture system (2, 3). Because of the central role of ubiquitin-dependent proteolysis in regulating fundamental cellular events such as cell division and apoptosis, many recent studies suggest a potential mechanism linking protein aggregation to cellular disregulation and cell death (2, 3). However, the execution mechanisms underlying the neuronal cell death mediated by pathogenic inclusions and proteasome inhibition remain poorly understood, especially regarding the genetic evidence involving unfolded proteins in neurotoxicity *in vivo*.

We used a technique for genetic screening in *Drosophila* to identify gene products that can cause neural death or degeneration (4, 5) and revealed that one of these gene products, a homologue of Sec61α translocon, plays a critical role in neural cell death and degeneration (H.K. and M.M., unpublished data). Protein-conducting channels of eukaryotic endoplasmic reticulum (ER) are composed of three transmembrane subunits: Sec61α, Sec61β, and Sec61γ (6–8), collectively termed a translocon. Translocons are known to be required for both protein import (for the translocation of membrane or secretory preproteins) and export [for ER-associated protein degradation (ERAD)] at the ER lumen (9–11). Eukaryotic cells have complex degradation machinery enabling elimination of misfolded or unassembled secretory proteins from the ER. These proteins are retained in the ER/pre-Golgi compartment until retrograde translocation (dislocation) from the ER to the cytoplasm delivers them to the ubiquitin-proteasome system in ERAD. This dislocation process is mediated by Sec61α together with Sec61β and Sec61γ. Many recent observations suggest that increased protein dislocation from the ER or inhibition of the ubiquitin-proteasome system may lead to the accumulation of ER-derived misfolded proteins in the cytosol, thereby contributing to the pathogenesis of several severe human diseases (9). Recently, *Drosophila* has been used to elucidate mechanisms of human neurodegenerative disease, including Alzheimer's, Parkinson's, and Huntington's diseases (12–14). Therefore, we examined the function of *Drosophila* Sec61α in the induction of neuronal cell death and degeneration, particularly during expanded polyglutamine-mediated neurotoxicity. Sec61α was found to be necessary for polyglutamine-induced neurodegeneration, and loss of Sec61α function in *Drosophila* reduced amounts of ubiquitinated protein accumulation induced by expanded polyglutamine. Our results suggest that the Sec61α translocon mediates protein deposition from the ER to the cytoplasm and that toxicity results from the proteasome's inability to degrade these proteins in the presence of expanded polyglutamine proteins.

Experimental Procedures

Fly Stocks. All general fly stocks and GAL4 lines were obtained from *Drosophila* stock centers. Fly culture and crosses were performed at 25°C. The *UAS-MJDtr-Q78* and *GMR-huntingtin120Q* flies were a gift from Nancy Bonini (University of Pennsylvania, Philadelphia) and Lary Zipursky (University of California, Los Angeles) (13, 14).

Histology. Flies were prepared for semithin sections and toluidine blue staining as described (15). All fluorescent labeling was examined with an Axioskop2plus fluorescence microscope (Zeiss) and LSM510 confocal microscope (Zeiss). For light microscopic images of the adult eye, flies were anesthetized and

Abbreviations: ER, endoplasmic reticulum; ERAD, ER-associated protein degradation; dsRNA, double-stranded RNA; UPR, unfolded protein response; MJD, Machado–Joseph disease; EGFP, enhanced GFP; PrP, prion protein.

†Present address: Department of Microbiology and Immunology, Stanford University School of Medicine, Fairchild Science Building D333, Stanford, CA 94305-5124.

**To whom correspondence should be addressed. E-mail: miura@mol.f.u-tokyo.ac.jp.

examined with a Nikon SMZ1000 microscope equipped with an AxioCam digital camera (Zeiss).

Plasmid Construction. An *DSec61α* fragment from an EST clone (LP02784) was inserted into *pUAST* and *pBSSK* to generate *pUAST-DSec61α* and *pBSSK-DSec61α*. A fragment for FLAG-tagged DSec61α amplified by PCR was inserted into *pUAST* (*pUAST-FLAG-DSec61α*) and *pCaspeR-hs* (*pCaspeR-hs-FLAG-DSec61α*). The *EGFP* fragment from *pCaspeR-hs-EGFP* (15) was inserted into *pBSSK* (*pBSSK-EGFP*). The fragments of *tNhtt-Q17-EGFP*, *tNhtt-Q60-EGFP*, and *tNhtt-Q150-EGFP* (16) were inserted into *pUAST* (*pUAST-htt17QEGFP*, *pUAST-htt60QEGFP*, and *pUAST-htt150QEGFP*, respectively) and *pCaspeR-hs* (*pCaspeR-hs-htt17QEGFP*, *pCaspeR-hs-htt60QEGFP*, and *pCaspeR-hs-htt150QEGFP*, respectively). A driver plasmid that expresses GAL4 under the control of the *actin5C* promoter (*pWAGAL4*), *pUAST-GFP*, and *pCaspeR-hs-lacZ* has been described (17, 18).

Cell Culture, Transfections, and Viability Assay. *Drosophila* S2 cells and neural cell line BG2-c6 (BG2 cells) (19) were cultured and transfected as described (18, 19). For a cell death assay, these cells were cultured in 24-well plates (1 10^5 cells per well) and transfected with various amounts of the indicated plasmids plus 2 ng of *pWAGAL4*, which expresses the GAL4 protein under the control of the *actin5C* promoter. In the RNA interference experiments, described amounts of double-stranded RNA (dsRNA) were transfected by the same procedure. At 24 h after transfection, cells were heat-shocked at 37°C for total 2 h, cultured at 27°C for 24 h, and then subjected to cell death assay as described (18). For a viability assay in *Drosophila* embryos, plasmids that can be driven by heat-shock promoter (*pCaspeR-hs* constructs) were dissolved in injection buffer (5 mM KCl in 0.1 mM phosphate buffer, pH 8.0) at 50 or 100 ng/μl. Embryos were collected within 30 min after egg laying at 25°C, dechorionated, and attached to a coverslip with double-stick tape. Embryos were then covered in halocarbon oil and injected at precellularized stage. Injection location was in the posterior domain extending from 50% to 75% egg length. The DNA solution was injected by a syringe. The injection volume ranged from 50 to 150 pL as determined by measuring the diameter of droplets injected into halocarbon oil. At 12 h after injection, embryos were heat-shocked at 37°C for 1 h and developed for 12 h, and hatched larvae were counted.

Immunoblotting. For detection of ubiquitinated proteins and FLAG-tagged or Myc-tagged proteins, S2 cells were cultured in six-well plates (5 10^5 cells per well) and transfected with various amounts of the indicated plasmids. At 24 h after transfection, the cells were lysed in SDS sample buffer. Fly eyes were carefully dissected from anesthetized flies and lysed in SDS sample buffer to assay for ubiquitinated proteins. All samples were separated by 10% SDS/PAGE and subjected to immunoblotting using an anti-ubiquitin mouse antibody (1:250, Stressgen Biotechnologies, Victoria, Canada), anti-myc mouse antibody (1:2,000, Invitrogen), anti-FLAG M2 antibody (1:1,000, Sigma), anti-β-tubulin E7 (1:500, Developmental Studies Hybridoma Bank, Iowa City), and an anti-mouse IgG-horseradish peroxidase antibody (1:1,000, Promega). The signals were visualized with ECL plus (Amersham Pharmacia).

Proteasome Activity. Proteasome activity was assessed in lysates of S2 cells by using synthetic peptide substrates linked to a fluorometric reporter, aminomethylcoumarin (20). S2 cells were cultured in 6-well plates (5 10^5 cells per well) and transfected with various amounts of the indicated plasmids. At 24 h after transfection, cells were collected, washed in PBS, and lysed in buffer H (20 mM Tris/20 mM NaCl/1 mM EDTA/5 mM β-mercaptoethanol, pH 7.6). Cell lysates were collected by centrifugation, and the supernatants were used for the determination of protein concentration and enzymatic activity by using Suc-LLVY-MCA (Peptide Institute, Osaka) as described (20).

RNA Interference in *Drosophila* Cells. For the production of synthesized dsRNA, the indicated cDNA fragments flanking both the T7 and T3 promoter sequences were amplified by PCR from each *pBSSK* plasmid (as described above) with the specific primers. The amplified fragments were purified and served as templates for RNA synthesis using T7 or T3 RNA polymerase (Promega) by standard protocols. The RNAs were ethanol-precipitated, dissolved in water, quantified, and mixed for annealing in equal quantities by heating for 10 min at 68°C and cooling to 37°C for 30 min. The resulting dsRNAs were checked to verify their purity and size on agarose gels. For generating a head-to-head inverted repeat construct, a fragment (nucleotides 101–1000 of the ORF) fused with *Bgl*II and *Xba*I sites was inserted into the *Bgl*II/*Xba*I site of *pUAST*. Next, another fragment (nucleotides 201–1000 of ORF) fused to *Bgl*II and *Eco*RI sites was inserted into the *Eco*RI/*Bgl*II site of the same plasmid to generate *pUAST-DSec61α dsRNA*. In RNA interference experiments, each dsRNA material was transfected into BG2 or S2 cells by using CellFectin (GIBCO) as described above.

***DSec61α* Mutant Fly.** As the candidate mutant lines for the *DSec61α* gene, the *P560(l(2)k04917)* and *EP(2)2567 P* element strains were identified from the Berkeley *Drosophila* Genome Project. The *P* element insertion sites in these lethal lines were found to reside in the first intron of the *DSec61α* gene. The lethality reverted when the inserted *P* element of *P560* was excised. *P* element revertants were generated by standard genetic techniques, and the association of the observed phenotype with the *P* element insertion was confirmed by excision of the *P* element: one excision line of *P560*, $DSec61\alpha^{P560ex25}$, could not improve the expanded polyglutamine-induced eye degeneration (Fig. 5, which is published as supporting information on the PNAS web site, www.pnas.org). The *P560* and *EP(2)2567* strains were putative hypomorphic alleles for *DSec61α*, because RT-PCR analysis revealed that the amount of mRNA for *DSec61α* was significantly reduced in larvae transheterozygous for these strains (data not shown). Thus, we designated these strains $DSec61\alpha^{P560}$ and $DSec61\alpha^{EP(2)2567}$.

Results

DSec61α Is Involved in Neural Cell Death Induced by Proteasome Inhibition. To elucidate the mechanisms of neural cell death including neurodegeneration, we developed a screen for genes involved in the neuronal cell death associated with neurodegeneration, involving the overexpression of individual genes throughout much of the *Drosophila* genome. Briefly, to identify neuronal cell death-related genes, we used misexpression fly strains, GS lines, that would misexpress unknown genes driven by GAL4 protein. In our screen we used a *rhodopsin 3-GAL4* (*rh3-GAL4*) line that expresses the GAL4 activator in a specific subset of postmitotic photoreceptor neurons in the adult, expecting that the *rh3-GAL4* line combined with GS lines would allow us to identify potential cell death genes of a type that could induce neuronal cell death in a cell-autonomous fashion. As a result of the screen of 5,000 fly strains, we identified and characterized the *endd2* gene, which encodes the *Drosophila* ortholog of Sec61α (DSec61α) located in ER, as a component of the neural cell death and degeneration pathways (H.K. and M.M., unpublished data). To understand the mechanisms of this cell death, we examined the role of DSec61α in neural cell death induced by various kinds of stimuli including the proteasome inhibitor lactacystin. In *Drosophila*, RNA interference has been shown to be an effective method to knock down specific targeted

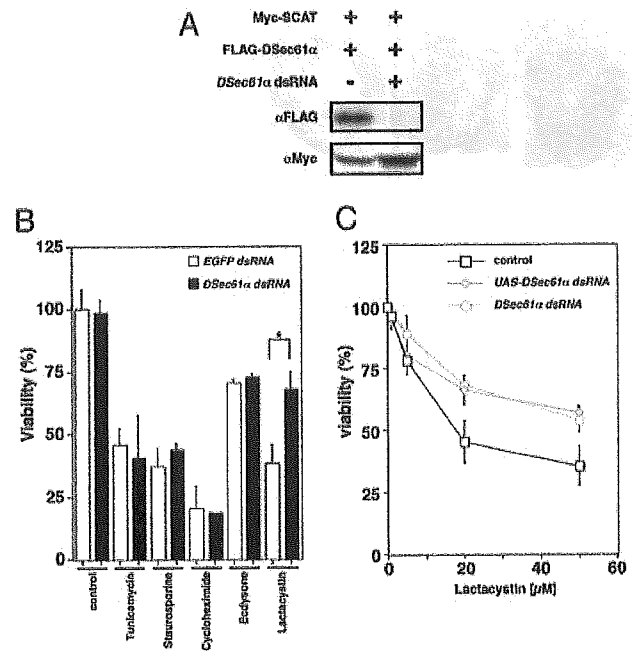

Fig. 1. DSec61α contributes to cell death induced by proteasome inhibition in Drosophila cells. (A) RNA interference experiments in Drosophila cells. The synthesized dsRNA or the dsRNA expressed as an extended hairpin-loop RNA by the UAS vector were used to knock down the DSec61α protein expression. Briefly, 200 ng each of UAS-FLAG-DSec61α, UAS-Myc-SCAT (used as a control), and pWAGAL4 were cotransfected with 25 ng of synthesized DSec61α dsRNA into Drosophila S2 cells. At 24 h after transfection, the cells were collected and subjected to immunoblotting using an anti-myc and anti-FLAG antibody. (B) The DSec61α gene is partially required for neural cell death induced by lactacystin, which inhibits proteasome activity in cells. dsRNA (25 ng of EGFP and DSec61α) was transfected into Drosophila BG2 neural cells. Twenty-four hours after transfection, 10 μg/ml tunicamycin, 1 μM staurosporine, 1 μg/ml cycloheximide, 10 μM ecdysone, and 20 μM lactacystin were added to the media. The cells were then incubated for 24 h, and the cell viability was determined. (C) Synthesized dsRNA (25 ng of DSec61α dsRNA) or dsRNA expression vector (10 ng of UAS-DSec61α dsRNA with 2 ng of pWAGAL4) was transfected into Drosophila S2 cells. Twenty-four hours after transfection, lactacystin was added to the media (1, 5, 20, and 50 μM). The cells were then incubated for 24 h more, and the cell viability was determined.

gene products (21–23) and was used in our experiments for the knockdown of DSec61α protein expression (Fig. 1*A*). Addition of lactacystin, a proteasome inhibitor, caused a severe reduction in cell viability that was partially alleviated through disruption of DSec61α (Fig. 1 *B* and *C*). This finding is in contrast to other drugs, including tunicamycin, an inhibitor of N-glycosylation that induces the rapid unfolded protein response (UPR), staurosporine, cycloheximide, and ecdysone, all of which caused cell death independently of DSec61α (Fig. 1*B*). Thus, these data indicate that DSec61α contributes to neural cell death induced by disruption of proteasome function.

Expanded Polyglutamine Provokes Proteasome Inhibition

A number of studies have focused on the potential role of protein aggregation and disruption of the proteasome proteolytic pathway in polyglutamine-mediated neurodegeneration (2, 3). Because our results suggested involvement of DSec61α in a cell death signaling pathway evoked by proteasome inhibition, we analyzed a possible connection between expanded polyglutamine-mediated toxicity and the DSec61α translocon protein. The expression of truncated versions of the pathogenic human *MJD/SCA3* gene or the human *Huntingtin* gene in postmitotic neurons elicits late-onset progressive degeneration and the loss of photoreceptor neurons in a manner largely independent of caspase-dependent

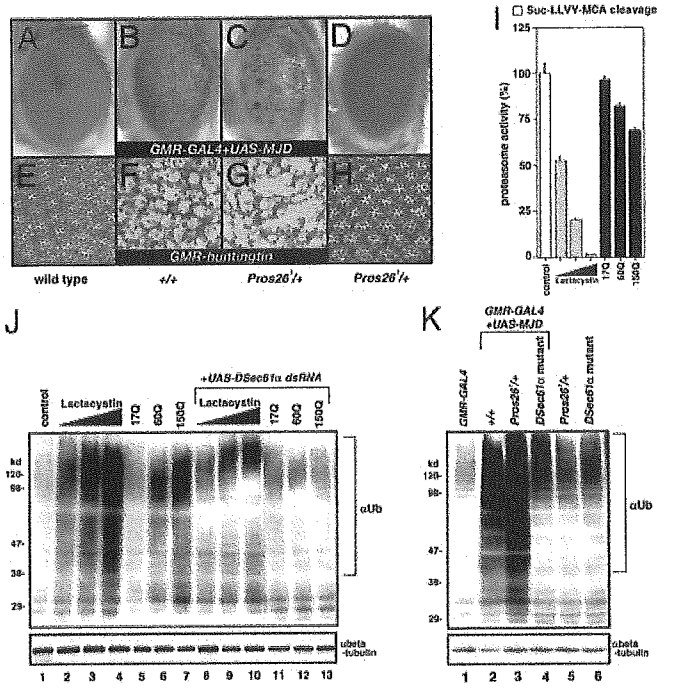

Fig. 2. The DSec61α translocon is required for the accumulation of undegraded proteins caused by expanded polyglutamine. (A–H) In the fly models for the polyglutamine diseases MJD and Huntington's disease, the partial loss of the 26S proteasome subunit clearly enhanced the phenotypes of neurodegeneration in the eye. Light microscopic (A–D) and semithin section (E–H) images of the compound eyes are shown (day 15 after eclosion). (Magnifications: 63.) The following genotypes are shown: w;GMR-GAL4 / (A and E), w;GMR-GAL4 / ;UAS-MJD(M)/ (B), w;GMR-GAL4 / ;UAS-MJD(M)/Pros26 (C), w; / ;Pros26 (D and H), w; / ;GMR-huntingtin120Q (F), and w; / ;GMR-huntingtin120Q/Pros26 (G). (I) Proteasome activity in Drosophila cells. Plasmids (800 ng) encoding the expanded polyglutamine tracts (httQ17, httQ60, and httQ150) were overexpressed in Drosophila S2 cells with 200 ng of driver plasmid pWAGAL4 . Other S2 cells were treated with lactacystin (1, 5, and 20 μM). The proteasome activities (a cleavage activity of Suc-LLVY-MCA; chymotrypsin-like) were measured 24 h after transfection. Enzymatic activity is expressed as the percentage of the activity in control lysates. (J) Immunoblotting of the cell lysates prepared in I with the anti-ubiquitin (αUb) antibody. In some cases, 30 ng of UAS-DSec61α dsRNA and 200 ng of driver plasmid pWAGAL4 were cotransfected. Similar amounts of protein were loaded, as determined by using an anti-β-tubulin (αbeta-tubulin) antibody. (K) The accumulation of ubiquitinated proteins induced by the expanded polyglutamine tracts in the Drosophila eye was remarkably reduced in flies that were transheterozygous for the mutant DSec61α allele. Eighteen fly eyes from each line of the indicated genotype (day 1 after eclosion) were carefully dissected and subjected to immunoblotting with an anti-ubiquitin (αUb) antibody. Similar amounts of protein were loaded, as determined with an anti-β-tubulin (αbeta-tubulin) antibody. The following genotypes are shown: w;GMR-GAL4 / (lane 1), w;GMR-GAL4 / ;UAS-MJD(M)/ (lane 2), w;GMR-GAL4 / ;UAS-MJD(M)/Pros26 (lane 3), w;GMR-GAL4 DSec61α^{P560}/DSec61$\alpha^{EP(2)2567}$;UAS-MJD(M)/ (lane 4), w; / ;Pros26¹/ (lane 5), and w;DSec61α^{P560}/DSec61$\alpha^{EP(2)2567}$; / (lane 6).

cell death pathways (13, 14). We first examined the correlation between polyglutamine-induced neural degeneration and the ubiquitin-proteasome function. In agreement with previous finding (24), reduced gene dosage of *Pros*26 (described below) clearly enhanced the neurodegeneration in flies expressing Machado–Joseph disease (MJD) protein or Huntingtin (Fig. 2 *A–H*). Similarly, overexpression of expanded polyglutamine reduced proteasome activity in a tract length-dependent manner in S2 cells and treatment of S2 cells with the proteasome inhibitor, lactacystin, blocked proteasome activity, resulting in the accumulation of ubiquitin conjugates (Fig. 2 *I* and *J*).

Furthermore, the accumulation of ubiquitin conjugates from whole eyes and S2 cells expressing expanded polyglutamine exhibited a stronger high-molecular-weight smear of ubiquitin immunoreactivity (Fig. 2*J* and *K*). The proteolytic machinery of regulated protein degradation is a large, multisubunit complex known as the 26S proteasome. This complex is made up of two components: a 20S core particle composed of four stacked heptameric rings and 19S regulatory complexes capping each end. *Drosophila Pros26*^{1} is missense mutations in the 20S proteasome subunits, β6. In a mutant heterozygous for this 26S proteasome subunit gene (*Pros26*^{1}/), the accumulation of ubiquitin conjugates from whole eyes expressing expanded polyglutamine was significantly enhanced (Fig. 2*K*). These data indicate that the mechanism underlying the neural degeneration induced by expanded polyglutamine tracts involves inhibition of proteasome function, which can lead to the accumulation of undegraded, ubiquitin-conjugated proteins.

DSec61α Is Involved in Polyglutamine-Induced Neural Cell Death and Degeneration. Like MJD/SCA3 or Huntingtin overexpression, DSec61α overexpression induced cell death and degeneration partially through a caspase-independent pathway that is distinct from that used by other known *Drosophila* killer proteins, Reaper and Hid (data not shown). The finding that DSec61α function is partially involved in a caspase-independent signaling pathway also suggests a possible connection between endogenous DSec61α protein and polyglutamine toxicity in neural tissues. To further explore this connection *in vivo*, we crossed lines expressing truncated MJD protein with an expanded polyglutamine tract (78 repeats) or Huntingtin with hypomorphic *DSec61α* mutants (*DSec61α*^{P560} and *DSec61α*$^{EP(2)2567}$). WT flies expressing expanded polyglutamine protein exhibited severe, progressive eye deterioration (Fig. 3 *A* and *B*), and extensive photoreceptor degeneration contributing to an unusual ommatidium morphology (Fig. 3 *D* and *E*). Strikingly, a reduced gene dosage of *DSec61α* significantly suppressed these phenotypes, ameliorating the loss of pigment (Fig. 3 *B* and *C*) and photoreceptor degeneration (Fig. 3 *E* and *F*). To confirm this suppression depended on the loss of function of *DSec61α* we generated a revertant and found it could not suppress the polyglutamine-mediated neurodegeneration (Fig. 5). Next, we overexpressed the first exon of human Huntingtin, containing expanded polyglutamine region (17, 60, and 150 repeats), fused to enhanced GFP (EGFP) (16), in the *Drosophila* neural cell line BG2. The level of polyglutamine aggregation, as indicated by the EGFP fluorescence, depended on the length of the overexpressed polyglutamine repeats (Fig. 3*G Top*) with a corresponding change in cell viability 72 h after transfection (Fig. 3*G Bottom*). Again, DSec61α was shown to be indispensable in this toxicity; although knockdown of DSec61α through cotransfection of *DSec61α* dsRNA did not affect the rate of aggregation (Fig. 3*G Middle*), neural cell death was significantly reduced (Fig. 3*G Bottom*). Similar results were seen when expanded polyglutamine-EGFP fusion proteins were overexpressed in *Drosophila* embryos. Direct injection of cDNA containing 150 polyglutamine repeats, but not shorter repeats, clearly exhibited many aggregate-like structures in embryos (Fig. 3*H*) and resulted in severe lethality of WT embryos (Fig. 3*I* and Table 1). This finding is in contrast to *DSec61α* mutant embryos in which expression of expanded polyglutamine did not significantly exert toxic effects on embryos (Fig. 3*I*). However, when DSec61α was coexpressed with polyglutamine in *DSec61α* mutant embryos, lethality was once again seen. This toxicity depended on coexpression of DSec61α and polyglutamine, as expression of DSec61α alone did not cause lethality (Table 1). Thus, DSec61α is involved in expanded polyglutamine-induced neural cell death and degeneration.

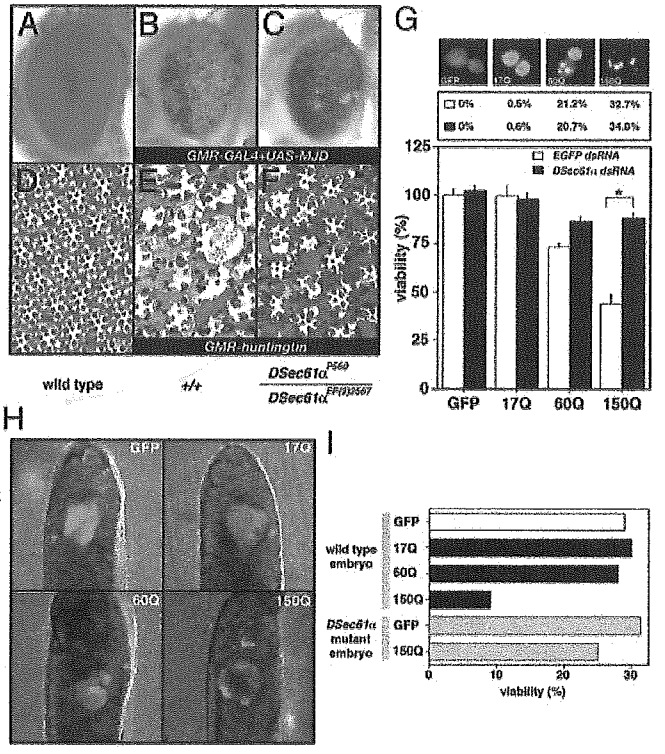

Fig. 3. The DSec61α translocon is involved in expanded polyglutamine-induced neural cell death and degeneration in *Drosophila*. (A–F) The degenerative eye phenotype of the different *Drosophila* models for polyglutamine disease was improved in mutants for the *DSec61α* gene. Light microscopic (A–C) and semithin section (D–F) images of the compound eyes are shown (day 30 after eclosion). (Magnifications: 100.) The following genotypes are shown: w;GMR-GAL4/ (A and D), w;GMR-GAL4/ ;UAS-MJD(M)/ (B), w;GMR-GAL4 DSec61α^{P560}/DSec61α$^{EP(2)2567}$;UAS-MJD(M)/ (C), w; / ;GMR-huntingtin120Q/ (E), and w;DSec61α^{P560}/DSec61α$^{EP(2)2567}$;GMR-huntingtin120Q/ (F). (G) The neural cell death induced by expanded polyglutamine tracts was attenuated in the *DSec61α* gene knockdown cells. (*Top*) Plasmids (200 ng of each type) encoding the expanded polyglutamine tracts with the first exon of human Huntingtin fused to EGFP (pUAST vectors) were overexpressed in *Drosophila* BG2 neural cells with 200 ng of driver plasmid pWAGAL4 . The fluorescence indicating GFP-positive cells was examined 24 h after transfection. (*Middle*) Plasmids (200 ng of each type) encoding the expanded polyglutamine tracts were cotransfected with 25 ng of synthesized dsRNA (EGFP or DSec61α) in *Drosophila* BG2 neural cells with 200 ng of driver plasmid pWAGAL4. The numbers indicate the percentages of the population of GFP-positive cells that contained fluorescent aggregates (EGFP dsRNA, E; DSec61α dsRNA, F). (*Bottom*) Plasmids (5 ng of each type) encoding the expanded polyglutamine tracts were cotransfected with 25 ng of synthesized dsRNA (EGFP or DSec61α) in *Drosophila* BG2 neural cells with 2 ng of driver plasmid pWAGAL4 , and cell viability was determined. (H and I) The aggregate-like structure was produced by expanded polyglutamine in *Drosophila* embryos, which affected viability of embryos. Three types of expanded polyglutamine tracts with the first exon of human Huntingtin fused to EGFP and 100 ng/μl pCaspeR-hs vectors were injected into *Drosophila* embryos (w^{1118} and DSec61α$^{EP(2)2567}$/DSec61α^{P560}). At 12 h after injection, embryos were heat-shocked at 37°C for 1 h and developed at 25°C for 12 h. The fluorescence indicating GFP-positive cells was examined 18 h after injection (H). And then the number of hatched larvae was counted (I).

Accumulation of Ubiquitinated Proteins by Expanded Polyglutamine Mediated by DSec61α. To gain insight into the mechanism by which the Sec61α translocon regulates polyglutamine-mediated neural degeneration, we focused on the function of DSec61α. We hypothesized that for polyglutamine tracts to exert a toxic effect, DSec61α must be able to dislocate potentially toxic proteins to the cytoplasm where the inhibited proteasome would no longer be able to degrade them. Interestingly, when the expression level

Table 1. DSec61α function is involved in polyglutamine-mediated toxicity in *Drosophila* embryos

Genotype	Injected gene(s)	Ratio of viable larvae, % (total N)
w^{1118}	hs-GFP	29.0 (178)
	hs-htt150Q	9.0 (187)
$DSec61\alpha^{EP(2)2567}/DSec61\alpha^{P560}$	hs-GFP hs-lacZ	31.3 (213)
	hs-htt150Q hs-lacZ	25.0 (203)
	hs-GFP hs-DSec61α wt	29.8 (196)
	hs-htt150Q hs-DSec61α wt	10.1 (208)

Precellularized embryos from WT (w^{1118}) or DSec61α mutant ($DSec61\alpha^{EP(2)2567}/DSec61\alpha^{P560}$) flies were injected with 100 ng/μl hs-GFP or hs-htt150Q in addition to 50 ng/μl hs-lacZ or hs-DSec61α wt and allowed to develop at 25°C. At 12 h after injection, embryos were heat-shocked at 37°C for 1 h and developed at 29°C for 12 h, and the numbers of hatched larvae were counted.

of *DSec61α* mRNA was down-regulated by treatment with dsRNA, the accumulation of ubiquitinated proteins induced by lactacystin in *Drosophila* cells was clearly reduced (compare Fig. 2*J*, lanes 2–4 and 8–10). Similar results were observed when expanded polyglutamine was overexpressed in S2 cells (compare Fig. 2*J* lanes 5–7 and 11–13). Furthermore, we observed a remarkable reduction of ubiquitinated proteins induced by expanded polyglutamine in the eyes of transheterozygous *DSec61α* mutants (compare Fig. 2*K*, lanes 2 and 4). Correlated with this observations, we examined the expression of *Drosophila BiP* (*dBiP*) in cells and fly embryos. The UPR directly correlates with the acute up-regulation of the molecular chaperone *BiP/GRP78*, and inhibition of ERAD in yeast induces the UPR induction (see *Supporting Text*, which is published as supporting information on the PNAS web site). As a result, the reduction of *DSec61α* caused the rapid induction of *dBiP* (Fig. 6, which is published as supporting information on the PNAS web site), indicative of rapid induction of the UPR, suggesting that loss of DSec61α may lead to a reduction of protein dislocation. Because severe reduction of *DSec61α* expression in $DSec61\alpha^{P560}/DSec61\alpha^{P560}$ fly or in cells transfected with higher amount of *DSec61α* dsRNA clearly induced more UPR but also cell death (Fig. 6 and Fig. 7, which is published as supporting information on the PNAS web site), the mild loss of Sec61α translocon may contribute to the improvement of polyglutamine-mediated neural degeneration. Therefore, the increase in ubiquitinated proteins in response to polyglutamine requires a functional DSec61α translocon.

Discussion

The present study provides some important insights into neural cell death and degeneration caused by protein aggregates and unfolded proteins. Many recent studies suggest that proteasome inhibition might be a common link between the different genetic triggers of neurodegenerative diseases, especially amyotrophic lateral sclerosis, Parkinson's disease, and polyglutamine disease (1). For example, one hypothesis for the etiology of Parkinson's disease is that subsets of neurons are vulnerable to a failure in proteasome-mediated protein turnover. Overexpression of mutant α-synuclein increases sensitivity to proteasome inhibitors by decreasing proteasome function, whereas overexpression of Parkin decreases sensitivity to proteasome inhibitors in a manner dependent on Parkin's ubiquitin-protein E3 ligase activity (25). It is obvious that proteasome-inhibition induces accumulation of undegraded proteins that can trigger some kind of signal for cell death and degeneration; however, an important unanswered question remains: from where do these undegraded proteins come? The ubiquitin-proteasome system degrades proteins derived from all cellular components including the ER. Our present observations suggest that one source of undegraded protein might be the ER, thereby providing genetic evidence implicating the ER as an important source of undegraded, toxic proteins.

We characterized the *Drosophila* ortholog of Sec61α (DSec61α), a component of the translocon that is involved in ERAD in neural cell death and degeneration pathways. Loss-of-function experiments for DSec61α revealed that the translocon contributes to the expanded polyglutamine-mediated neuronal toxicity and accumulation of ubiquitinated proteins caused by inhibiting the proteasome. These observations provide a possible mechanism for polyglutamine toxicity: expanded polyglutamine inhibits the ubiquitin-proteasome function, thereby leading to an accumulation of unfolded proteins in the cytosol. Furthermore, these unfolded proteins are likely dislocated through the Sec61α translocon and other protein dislocation machinery (Fig. 4). Supporting this idea, the AAA ATPase Cdc48/p97/VCP, which is also involved in the ERAD system mediated by Sec61α (26, 27), has recently been identified as a positive regulator of polyglutamine-mediated toxicity in *Drosophila*; loss of *Drosophila* Cdc48/p97/VCP can improve the neurodegenerative phenotypes induced by expanded polyglutamine (28). Moreover, reduction of DSec61α may not only inhibit the retrograde translocation of unfolded proteins from the ER, but also suppress the translocation of nascent secretory protein into the ER, leading to a decrease of undegraded proteins in the cytosol (Fig. 4). Additionally, it might be possible that acute UPR induction that is caused by loss of DSec61α regulates the amount of ubiquitinated protein. Because UPR

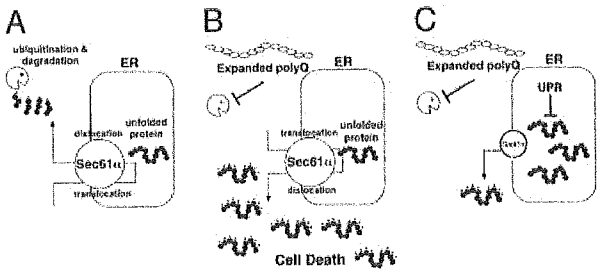

Fig. 4. A proposed model for Sec61α function in regulation of cell death. In normal cells (A), the translocation of secretory preproteins into ER is mediated by Sec61α. Unfolded proteins produced in ER are dislocated by Sec61α into the cytosol, which leads to protein degradation by the ubiquitin-proteasome system, a process known as ERAD. In contrast, when expanded polyglutamine is expressed, the proteasome activities are reduced. This inhibition of proteasome activity causes accumulation of ubiquitinated proteins because of an impaired ERAD system and continuous supply of these cytoplasmic undegraded proteins may induce cell death (B). However, a reduction of Sec61α function causes a decrease of translocated unfolded proteins into cytosol, resulting in accumulation of such proteins in ER. These unfolded proteins might be decreased by the UPR system in ER (C).

induction is correlated with up-regulation of molecular chaperone proteins (e.g., BiP/GRP78), this will lead to reduction of unfolded proteins in ER. Sequentially, the amount of unfolded proteins that should be dislocated into cytosol by ERAD system is decreased, resulting in significant reduction of ubiquitinated proteins that can contribute to polyglutamine-mediated toxicity. UPR may also reduce the expression of proteins in the cell and eventually reduce the level of ubiquitinated proteins. However, it is still less effective to improve the phenotypes of polyglutamine-expressing flies by loss of DSec61α function, suggesting that the accumulation of ubiquitinated protein, added to the nuclear functions of expanded polyglutamine such as transcriptional repression, may be a partial contributor to the degeneration, and not solely responsible for polyglutamine-mediated degeneration. Thus, such an entire translocation/dislocation system of unfolded proteins through the ER might contribute to accumulation of undesirable proteins in cells when proteasome activity is inhibited in specific neurodegenerative disease conditions.

Many recent observations suggest that there could be specific kinds of toxic proteins in whole amounts of undegraded proteins. The Pael receptor, a substrate of the ubiquitin ligase Parkin, is proposed to be degraded by ERAD and exhibits neural toxicity when the ubiquitin-proteasome system is impaired; this cell death may be partially accompanied by cytosolic Pael receptor aggregates (29). Because accumulation of mutant forms of α-synuclein or loss of Parkin E3 ligase activity causes inhibition of ubiquitin-proteasome system (25), it might be possible that unfolded Pael receptor is dislocated by the Sec61α translocon from the ER in dopaminergic neurons in Parkinson's disease. Another example stems from changes in prion protein (PrP) folding that are associated with fatal neurodegenerative disorders such as bovine spongiform encephalopathy, scrapie, and Creutzfeldt–Jakob disease. However, the neurotoxic species is unknown. Like other proteins that traffic through the ER, misfolded PrP is retrograde transported to the cytosol for degradation by proteasomes. The transmembrane form of the prion protein (^{Ctm}PrP) is rapidly degraded by the ubiquitin-proteasome system under normal conditions (30, 31); however, under certain circumstances, the specific isoform of PrP is dislocated from the ER, and accumulation of even small amounts of cytosolic PrP leads to neurotoxicity in cultured cells and transgenic mice (32, 33). Similarly the dislocation of these neurotoxic PrPs might be carried through the Sec61α translocon. These lines of evidence show that the ERAD machinery must be tightly regulated to avoid cellular disorders, while maintaining efficient proteasome function, otherwise misfolded or unassembled potentially toxic secretory proteins may accumulate in the cytosol. Thus, considering the importance of the DSec61α translocon in these processes, specific regulators may prove to be valuable therapeutic tools for the treatment of several severe human neurodegenerative diseases.

We are grateful to R. Akai for technical support, N. Nukina, Y. Hiromi, K. Ui-Tei, N. Bonini, and L. Zipursky, for materials and flies, the Developmental Studies Hybridoma Bank for antibody, the Berkeley *Drosophila* Genome Project for providing various reagents and information, and the Bloomington Stock Center for fly stocks. We are also grateful to N. Bence, N. Nukina, R. Takahashi, and R. Schekman for valuable discussions. This work was supported in part by grants from the Japanese Ministry of Education, Science, Sports, Culture, and Technology (to H.O. and M.M.), Core Research for Evolutional Science and Technology (CREST), Japan Science and Technology Corporation (to H.O.), and a RIKEN Bioarchitect Research Grant (to M.M.). T.I. is a research fellow of the Japan Society for the Promotion of Science. E.K. is a research fellow of the Junior Research Associate Program, RIKEN. H.K. is a research fellow of the Special Postdoctoral Researchers Program, RIKEN.

1. Sherman, M. Y. & Goldberg, A. L. (2001) *Neuron* 29, 15–32.
2. Bence, N. F., Sampat, R. M. & Kopito, R. R. (2001) *Science* 292, 1552–1555.
3. Jana, N. R., Zemskov, E. A., Wang, G. H. & Nukina, N. (2001) *Hum. Mol. Genet.* 10, 1049–1059.
4. Kanuka, H. & Miura, M. (2002) *Cell Death Differ.* 9, 231–233.
5. Toba, G., Ohsako, T., Miyata, N., Ohtsuka, T., Seong, K. H. & Aigaki, T. (1999) *Genetics* 151, 725–737.
6. Gorlich, D. & Rapoport, T. A. (1993) *Cell* 75, 615–630.
7. Hanein, D., Matlack, K. E., Jungnickel, B., Plath, K., Kalies, K. U., Miller, K. R., Rapoport, T. A. & Akey, C. W. (1996) *Cell* 87, 721–732.
8. Schekman, R. (1996) *Cell* 87, 593–595.
9. Plemper, R. K. & Wolf, D. H. (1999) *Trends Biochem. Sci.* 24, 266–270.
10. Pilon, M., Schekman, R. & Romisch, K. (1997) *EMBO J.* 16, 4540–4548.
11. Zhou, M. & Schekman, R. (1999) *Mol. Cell* 4, 925–934.
12. Fortini, M. E. & Bonini, N. M. (2000) *Trends Genet.* 16, 161–167.
13. Warrick, J. M., Paulson, H. L., Gray, B. G., Bui, Q. T., Fischbeck, K. H., Pittman, R. N. & Bonini, N. M. (1998) *Cell* 93, 939–949.
14. Jackson, G. R., Salecker, I., Dong, X., Yao, X., Arnheim, N., Faber, P. W., MacDonald, M. E. & Zipursky, S. L. (1998) *Neuron* 21, 633–642.
15. Kanuka, H., Sawamoto, K., Inohara, N., Matsuno, K., Okano, H. & Miura, M. (1999) *Mol. Cell* 4, 757–769.
16. Wang, G. H., Mitsui, K., Kotliarova, S., Yamashita, A., Nagao, Y., Tokuhiro, S., Iwatsubo, T., Kanazawa, I. & Nukina, N. (1999) *NeuroReport* 10, 2435–2438.
17. Usui, T., Shima, Y., Shimada, Y., Hirano, S., Burgess, R. W., Schwarz, T. L., Takeichi, M. & Uemura, T. (1999) *Cell* 98, 585–595.
18. Igaki, T., Kanuka, H., Inohara, N., Sawamoto, K., Nunez, G., Okano, H. & Miura, M. (2000) *Proc. Natl. Acad. Sci. USA* 97, 662–667.
19. Ui, T. K., Sato, S., Miyake, T. & Miyata, Y. (1996) *Neurosci. Lett.* 203, 191–194.
20. Wojcik, C. & DeMartino, G. N. (2002) *J. Biol. Chem.* 277, 6188–6197.
21. Clemens, J. C., Worby, C. A., Simonson, L. N., Muda, M., Maehama, T., Hemmings, B. A. & Dixon, J. E. (2000) *Proc. Natl. Acad. Sci. USA* 97, 6499–6503.
22. Hammond, S. M., Bernstein, E., Beach, D. & Hannon, G. J. (2000) *Nature* 404, 293–296.
23. Kennerdell, J. R. & Carthew, R. W. (2000) *Nat. Biotechnol.* 18, 896–898.
24. Fernandez, F. P., Nino, R. M., de Gouyon, B., She, W. C., Luchak, J. M., Martinez, P., Turiegano, E., Benito, J., Capovilla, M., Skinner, P. J., *et al.* (2000) *Nature* 408, 101–106.
25. Petrucelli, L., O'Farrell, C., Lockhart, P. J., Baptista, M., Kehoe, K., Vink, L., Choi, P., Wolozin, B., Farrer, M., Hardy, J. & Cookson, M. R. (2002) *Neuron* 36, 1007–1019.
26. Ye, Y., Meyer, H. H. & Rapoport, T. A. (2001) *Nature* 414, 652–656.
27. Jarosch, E., Taxis, C., Volkwein, C., Bordallo, J., Finley, D., Wolf, D. H. & Sommer, T. (2002) *Nat. Cell Biol.* 4, 134–139.
28. Higashiyama, H., Hirose, F., Yamaguchi, M., Inoue, Y. H., Fujikake, N., Matsukage, A. & Kakizuka, A. (2002) *Cell Death Differ.* 9, 264–273.
29. Imai, Y., Soda, M., Inoue, H., Hattori, N., Mizuno, Y. & Takahashi, R. (2001) *Cell* 105, 891–902.
30. Hegde, R. S., Mastrianni, J. A., Scott, M. R., DeFea, K. A., Tremblay, P., Torchia, M., DeArmond, S. J., Prusiner, S. B. & Lingappa, V. R. (1998) *Science* 279, 827–834.
31. Yedidia, Y., Horonchik, L., Tzaban, S., Yanai, A. & Taraboulos, A. (2001) *EMBO J.* 20, 5383–5391.
32. Ma, J., Wollmann, R. & Lindquist, S. (2002) *Science* 298, 1781–1785.
33. Ma, J. & Lindquist, S. (2002) *Science* 298, 1785–1788.

ACADEMIC PRESS

Available online at www.sciencedirect.com

SCIENCE DIRECT®

Experimental Cell Research 291 (2003) 83–90

Experimental Cell Research

www.elsevier.com/locate/yexcr

Growth and differentiation potential of main- and side-population cells derived from murine skeletal muscle

Tetsuro Tamaki,[a,*] Akira Akatsuka,[b] Yoshinori Okada,[b] Yumi Matsuzaki,[d] Hideyuki Okano,[d] and Minoru Kimura[c]

[a] *Department of Physiology, Division of Human Structure and Function, Tokai University School of Medicine, Bohseidai, Isehara, Kanagawa 259-1193, Japan*

[b] *Laboratory for Structure and Function Research, Tokai University School of Medicine, Bohseidai, Isehara, Kanagawa 259-1193, Japan*

[c] *Department of Molecular Life Science, Tokai University School of Medicine, Bohseidai, Isehara, Kanagawa 259-1193, Japan*

[d] *Department of Physiology, Keio University School of Medicine, 35 Shinanomachi, Shinjyuku-ku, Tokyo 160-8582, Japan*

Received 14 March 2003, revised version received 19 June 2003

Abstract

Skeletal muscle-derived CD34+/45− (Sk-34) cells were identified as a new candidate for stem cells. However, the relationship between Sk-34 cells and side-population (SP) cells is unknown. Here, we demonstrate that Sk-34 cells prepared from murine skeletal muscles consist wholly of main-population (MP) cells. The Sk-34 cells included only a few SP cells (1:1000, SP:MP). Colony-forming units of Sk-34 cells of both SP and MP possessed the same potential to differentiate into adipocytes, endothelial, and myogenic cells and showed the same colony-forming activity (1.6%). In addition, the colony-forming units of the CD34−/45− (double negative: DN) population were found to begin CD34 expression and to possess the potential to differentiate into myogenic and endothelial cells. We also found that expression of CD34 antigen precedes MyoD expression during the myogenic process of DN cells. Furthermore, both Sk-34 and DN cell populations were mostly negative for CD73 (93–95%), whereas the CD45+ cell population was >25% positive for CD73, and this trend was also seen in bone marrow-derived CD45+ cells. These results indicate that the MP cell population is about 99.9% responsible for the reported in vitro myogenic-endothelial responses of skeletal muscle-derived cells.

Keywords: CD34; CD45; Side-population cells; Main-population cells; Endothelial cells; MyoD; CD73; Myoblast; Bone marrow; Stromal cell

Introduction

In order to open new pathways for tissue reconstitution therapy via cell transplantation, researchers continue to seek more convenient sources of stem cells. Several tissue-specific stem cells have been identified in adult brain [1,2], bone marrow [3,4], and skeletal muscle [5,6]. Skeletal muscle is the largest organ in the body, comprising about 40–50% of total body mass, and presumably, it allows donor cells to be obtained relatively easily and safely.

Classically, myoblasts in postnatal muscle have been considered to be derived from satellite cells located between the plasma membrane and the basal lamina of muscle fibers. More recently, hematopoietic and myogenic stem cell populations in the muscle, called side population (SP) cells, have been purified based on the efflux of the fluorescent dye Hoechst 33342 [5,6]. SP cells were shown to be clearly distinct from satellite cells in mutant mice lacking Pax-7, which exhibited a complete absence of satellite cells, while a normal population of SP cells was present [7].

In a recent study, we also identified "myogenic-endothelial" progenitor cell populations residing in the interstitial spaces of skeletal muscle by immunohistochemistry and immunoelectron microscopy based on an expression of CD34 antigen [8]. We characterized these cells using fluorescence-activated cell sorting (FACS) on the basis of cell surface antigen expression, and sorted them as a CD34+ and CD45− fraction from enzymatically isolated cells. Cells in the CD34+/CD45− fraction (designated Sk-34

* Corresponding author. Fax: +81-463-95-0961.
E-mail address: tamaki@is.icc.u-tokai.ac.jp (T. Tamaki).

0014-4827/$ – see front matter © 2003 Elsevier Inc. All rights reserved.
doi:10.1016/S0014-4827(03)00376-8

cells) were ~94% positive for Sca-1 and mostly negative (<3% positive) for CD14, 31, 49, 144, c-kit, and FLK-1. This demonstrates that Sk-34 cells are not committed endothelial progenitors because endothelial progenitor cells are positive for CD31, FLK-1, and CD144 (VE-cadherin) as well as for Sca-1 [9–11]. However, Sk-34 cells formed colonies in clonal cell culture, and colony-forming units (CFU) displayed the potential to differentiate into adipocytes, endothelial, and myogenic cells. Furthermore, Sk-34 cells fully differentiated into vascular endothelial cells and skeletal muscle fibers in vivo after transplantation. However, immediately after sorting, Sk-34 cells expressed c-met mRNA, but did not express any other myogenic cell-related mRNA, such as MyoD, myf-5, myf-6, myogenin, M-cadherin, Pax-3, and Pax-7. After culturing for 3 days, however, these cells expressed mRNA for all myogenic markers [8]. Interestingly, both the Sk-34 and the CD34−/45− (double negative: DN) cell fractions also expressed Bcrp1/ABCG2 mRNA, which has been shown to be sufficient to confer the "SP phenotype" [12]. Thus, it was suggested that at least some of the muscle SP cell activity described by Gussoni et al. [5] and Jackson et al. [6] might be attributed to the behavior of Sk-34 cells.

The aim of the current study was to clarify the relationship between SP cells and Sk-34 cells derived from the skeletal muscle. The growth and differentiation potentials of SP-Sk-34, MP-Sk-34, SP-DN, and MP-DN fractions were compared using clonal cell culture, and were characterized by immunocytochemistry and flow cytometry.

Materials and methods

Mouse strain

C57BL/6 mice were used for all cell cultures, immunocytochemistry, and flow cytometric characterizations.

Cell purification and characterization

Interstitial cells were extracted from entire muscles of the thigh and lower legs (tibialis anterior, extensor digitorum longus, soleus, plantaris, gastrocnemius, and quadriceps femoris) of 3- to 8-week-old mice using an isolation method for intact, living individual muscle fibers associated with satellite cells, as described previously [13]. Entire muscles were treated with 0.1% collagenase type IA (Sigma-Aldrich, Tokyo, Japan) in Dullbecco's modified Eagle's medium (DMEM) containing 10% fetal calf serum (FCS) with gentle agitation for 2 h at 37°C. Extracted cells were filtered through a 70-, 40-, and then a 20-μm nylon mesh, washed, and resuspended at 10^6 cells/ml in Hanks balanced salt solution (HBSS, GIBCO) containing 10% FCS and 10 mM Hepes. Hoechst 33342 (Sigma-Aldrich) was added to a final concentration of 5 μg/ml and the suspension was incubated for 90 min at 37°C. After Hoechst staining, cells were centrifuged, resuspended in cold HBSS, and then stained with fluorescein isothiocyanate (FITC)-conjugated anti-mouse CD34 (RAM34) and phycoerythrin (PE)-conjugated anti-mouse CD45 (30-F11). Cell analysis and sorting were performed using a triple laser VantageSE (Becton Dickinson, CA). Hoechst 33342 was excited at 350 nm, and fluorescence emission was detected using 405/BP30 and 585/BP20 optical filters against Hoechst blue and Hoechst red, respectively. A 555-nm-long pass dichroic mirror (Omega Optical Inc.) was used to separate emission wavelengths. Both Hoechst blue and red fluorescence were shown using a 488-nm Argon laser, and live cells were counted after cells positive for PI (propidium iodide) were excluded. After collecting 10^5 events, MP and SP populations were defined, as described previously [14]. The muscle SP cell population was confirmed by addition of 50 μM verapamil. Biotin-conjugated anti-mouse CD34 and streptavidin-APC and FITC- and PE-conjugated CD45 were used for the flow cytometric analysis of enzymatically extracted cells (EECs) and cultured Sk-34 and DN cells. All antibodies were purchased from Pharmingen (San Diego, CA). PE-conjugated Sca-1 (stem cell antigen) and CD73 (ecto-5′-nucleotidase) were also used to compare the characteristics between fractionated skeletal muscle-derived cells and bone marrow-derived mononuclear cells. In this respect, we obtained nucleated whole bone marrow cells from femurs of the same mice that were used for muscle analysis. Nucleated bone marrow cells were prepared by suspension in Histopaque 1083 (Sigma, St. Louis, MO) and used as a positive control in CD73 staining.

Clonal cell culture

Purified CD34+/45− cells (Sk-34) were plated in Methocult GFH4434V (StemCell Tech., Vancouver, Canada) complete methylcellulose medium and incubated in humidified atmosphere at 37°C in 5% CO_2. All cultures were performed in quadruplicate and scored at 14 days of culture using an inverted microscope. The growth potential of purified CD34−/45− (Sk-DN) cells was also determined using a clonal cell culture system based on a human collagen gel (CollagenCult H4742, StemCell Tech.) with 10 ng/ml bFGF and 20 ng/ml EGF.

Immunostaining

The specific cellular composition of each colony was determined by staining with monoclonal anti-MyoD (5.8A, Dako), anti-CD34 (RAM34) antibody, and fluorescein-labeled Isolectin B_4 (Griffonia Simplicifolia Lectin I, Vector Lab., Burlingame, CA), and evaluating uptake of acetylated low-density lipoprotein labeled with 1,1′-dioctadecyl-3,3,3′,3′-tetramethylindocarbocyanine perchlorate (DiI-Ac-LDL, Biomedical Technologies Inc., Stoughton, MA).

When staining for putative myogenic colonies in methylcellulose, each colony was manually extracted using a fine-tip glass pipette and then fixed with 4% paraformaldehyde/0.05 M phosphate buffer (4% PFA/PB) for 10 min. Cells were subjected to cytospin (1000 rpm) and then stained with monoclonal anti-MyoD. For sphere-forming cells in collagen gel, cells were resuspended in 0.1% collagenase (10 min at 37°C) and fixed with 4% PFA/PB. Cells were then subjected to cytospin and stained. Immunoreactions were visualized with streptavidin-biotin complex and 3,3-diaminobenzidine (DAB; Wako Pure Chemical, Osaka, Japan) and 4-chloro-1-naphthol (Wako). For the remaining adhesive and spreading cells in methylcellulose medium, the medium containing methylcellulose was washed out by DMEM containing 5% FCS, and the cells were cultured in DMEM containing 10 μg/ml DiI-Ac-LDL with 5% FCS for 3 h. The medium was then changed to DMEM containing 5 μg/ml Isolectin B_4 with 5% FCS, and cells were incubated for 15 min. After labeling with Isolectin B_4, cultures were washed with PBS, fixed using 10% formaldehyde neutral buffer solution, and stained with oil red O, a marker of lipid deposition. Flow cytometric analysis was also performed for the total Sk-34 and DN cells (a floating and/or weakly attached cell population and an adhesive, spreading cell populations) at 10 days of culture. For this purpose, an adhesive, spreading cell populations were resuspended by 0.05% trypsin solution containing 0.53 mM EDTA.

Results

MP and SP population in the enzymatically extracted cells

To clarify the relationship between SP cells and Sk-34 cells, we sorted SP and MP cells using Hoechst dye efflux [14], and further divided the two populations based on expression of cell-surface antigens CD34 and CD45. The typical pattern of isolation and characterization of muscle MP and SP fractions from EECs is shown in Fig. 1. The fraction of SP cells was small (0.08% of total cells), whereas MP cells accounted for 93% of total cells (Figs. 1A, C, and D). Both MP and SP fractions were stained for CD34 and CD45 to divide them into four subpopulations: CD34−/45+, CD34+/45+, CD34+/45−, and CD34−/45− (Figs. 1B and C). The SP cells were about 58% CD34+/45− (Sk-34), 36% CD34−/45− (DN), and the remaining 6% were in the CD45-positive fractions (CD34−/45+ and CD34+/45+)(Figs. 1C and D). In the case of MP cells, there were about 71% in Sk-34, 18% in DN, and the remaining 10% were in the CD45+ fractions. The number of MP-Sk-34 cells was about 1000-fold higher than the number of SP-Sk-34 cells (Fig. 1D). The number of MP-DN cells was also about 360 fold higher than SP-DN cells (Fig. 1D).

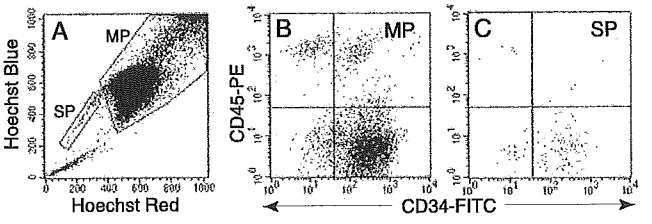

D	MP		SP	
Total	93.0±0.2		0.08±0.02	
34-/45+	4.6±1.3	(4.4±1.5)	<0.01	(0.8±0.7)
34+/45+	6.5±1.8	(6.0±1.8)	<0.01	(5.5±2.1)
DN	21.3±8.2	(18.4±6.9)	0.06±0.02	(36.0±11)
34+/45-	78.8±6.5	(71.2±4.9)	0.08±0.01	(57.8±9.7)

Fig. 1. Isolation and characterization of muscle MP and SP cells (A). MP and SP cells were further characterized by CD34 and CD45 (B, C). Both populations were divided into four subpopulations: CD34−/45+, 34+/45+, 34+/45− (Sk-34), and 34−/45− (DN). The percentage of total MP and SP in each fraction is shown in D. Values are calculated based on total events in A and expressed as mean ± SE for five trials. In parentheses, the mean frequency (%) of the four subpopulations in the MP and SP gate (mean ± SE) is shown (D).

Growth and differentiation characteristics, MP vs SP cells

To determine the growth characteristics and multilineage differentiation of purified SP-Sk-34 and MP-Sk-34 cells in vitro, we performed clonal cell culture in a semisolid medium. Both cell types began to form colonies within 5–7 days when cultured in medium containing methylcellulose (Figs. 2A and B). Some of these colonies formed sphere-like shapes (Figs. 2C and D). As the number of cells gradually increased, two distinct populations of cells were seen in colonies after 7–10 days: a floating and/or weakly attached cell population and an adhesive, spreading cell population. This is one of the typical characteristics of Sk-34 cells [8]. Both cell populations continuously increased their numbers and showed spontaneous, intermittent contractions. Numerous myotubes were also observed in the colony after 14 days of culture (Figs. 2E–H).

To characterize the cells composing these colonies in MP-Sk-34 and SP-Sk-34 cells after 10 days of culture, floating and/or weakly attached cells in individual colonies were picked up by micropipette, subjected to cytospin preparation, and stained for MyoD. The majority of these cells were strongly or weakly positive for MyoD (Figs. 2I and J). Expression of MyoD was relatively low in larger cells. Interestingly, a few cells, typically smaller cells, still expressed CD34 while coexpressing MyoD (Figs. 2K and L). Most of adhesive cell populations of MP- and SP-Sk-34 demonstrated uptake of DiI-Ac-LDL and were positive for Isolectin B_4 (Fig. 2M–O; MP and 2Q–S; SP). In addition, the total Sk-34 cells after 10 days of culture showed totally CD45 negative (Fig. 2U). Thus, it was considered that the adhesive cell populations demonstrating uptake of DiI-Ac-LDL and positive for Isolectin B_4 were endothelial cells.

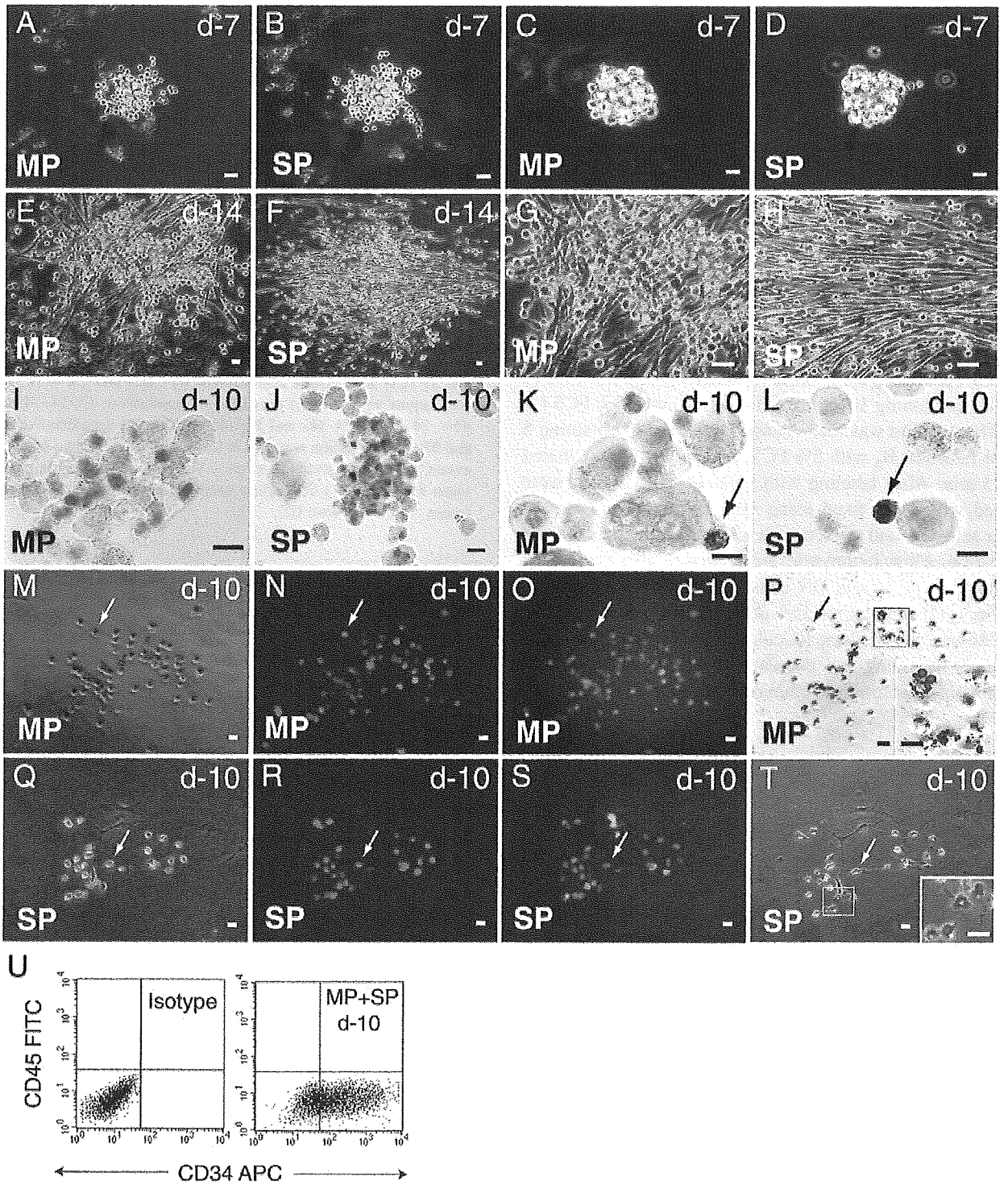

Fig. 2. Growth and differentiation of MP-Sk-34 and SP-Sk-34 cells in vitro. Colonies derived from each population after 7 days (A–D), 10 days (I–T), and 14 days (E–H) under the same culture conditions are shown. Typically, colonies were composed of floating and/or weakly attached large round cells and adherent spreading cells (A, B). Some colonies became roughly spherical (C, D). After 14 days of culture, numerous myotubes were formed in colonies of both populations (E, F). Panels G and H are higher magnification views of E and F. In cytospin preparations, the majority of weakly attached cell populations expressed MyoD after 10 days of culture (I, J, brown reaction), and note that a few small round cells coexpressed MyoD (brown) and CD34 (K, L, dark purple, arrow). Adherent cells remaining at the bottom of the plate, after washing the semisolid medium with the floating and/or weakly attached cells, are shown in (M–T). Most of these cells demonstrated DiI-Ac-LDL uptake and were positive for Isolectin B_4 (M–O and Q–S), and several cells showed oil droplet-like staining typical of fat cells (P, T). The insets of P and T show higher magnification views of the region outlined in the panel. Arrows in M–P and Q–T show the same cell in the MP and SP colonies. Resuspended total cells in Sk-34 cell cultured at 10 days showed totally CD45 negative (U). Colony-forming activity (%) of MP-Sk-34 and SP-Sk-34 cells was 1.6 ± 0.08 and 1.6 ± 0.07. Bars = 10 μm.